



# Calphad-type assessment of the FeNbNi ternary system

Muriel Mathon, Damien Connetable, Bo Sundman, Jacques Lacaze

## ► To cite this version:

Muriel Mathon, Damien Connetable, Bo Sundman, Jacques Lacaze. Calphad-type assessment of the FeNbNi ternary system. Calphad, 2009, 33 (1), pp.136-161. 10.1016/j.calphad.2008.10.005 . hal-00690488

**HAL Id: hal-00690488**

**<https://inria.hal.science/hal-00690488>**

Submitted on 10 Dec 2021

**HAL** is a multi-disciplinary open access archive for the deposit and dissemination of scientific research documents, whether they are published or not. The documents may come from teaching and research institutions in France or abroad, or from public or private research centers.

L'archive ouverte pluridisciplinaire **HAL**, est destinée au dépôt et à la diffusion de documents scientifiques de niveau recherche, publiés ou non, émanant des établissements d'enseignement et de recherche français ou étrangers, des laboratoires publics ou privés.



## Open Archive Toulouse Archive Ouverte (OATAO)

OATAO is an open access repository that collects the work of Toulouse researchers and makes it freely available over the web where possible.

This is an author-deposited version published in: <http://oatao.univ-toulouse.fr/>  
Eprints ID: 3772

**To link to this article:** DOI:10.1016/j.calphad.2008.10.005  
URL <http://dx.doi.org/10.1016/j.calphad.2008.10.005>

To cite this version: Mathon, Muriel and Connétable, Damien and Sundman, Bo and Lacaze, Jacques ( 2009) *Calphad-type assessment of the FeNbNi ternary system*. Calphad , vol.33 (1). pp. 136-161. ISSN 0364-5916

Any correspondence concerning this service should be sent to the repository administrator: [staff-oatao@inp-toulouse.fr](mailto:staff-oatao@inp-toulouse.fr)

# Calphad-type assessment of the Fe–Nb–Ni ternary system

Muriel Mathon, Damien Connétable, Bo Sundman, Jacques Lacaze\*

CIRIMAT, ENSIACET, UMR CNRS/UPS/INPT 5085, 118 Rte de Narbonne, 31077 Toulouse Cedex 4, Toulouse, France

## A B S T R A C T

This paper presents a Calphad-type thermodynamic database for the Fe–Nb–Ni system. The stable phases in this ternary system are liquid, fcc\_A1, bcc\_A2, C14 Laves, D0<sub>a</sub>, D8<sub>5</sub> and L1<sub>2</sub>\_fcc but we took also into account the C15 Laves and the metastable D0<sub>22</sub> phase because of their engineering interest. Available optimizations of the unary and binary systems were selected from the literature with the constraint that the Gibbs energy descriptions must be compatible. The only amendment needed to the selected assessments concerned the parameters for the D8<sub>5</sub> in the Fe–Nb system. In addition, ab-initio calculations have been performed using the VASP in order to help with estimating enthalpies of formation of some binary end members of the intermetallic compounds. The optimization of the Fe–Nb–Ni ternary system was performed using mostly experimental data available in the literature.

**Keywords:**  
Fe–Nb–Ni system  
Assessment  
Ab-initio  
Magnetism  
CALPHAD

## 1. Introduction

This work was initiated as part of a study devoted to the control of precipitation during processing of Inconel 718, a Ni-superalloy used in particular to manufacture disks for aeronautic and power turbines. Its good mechanical properties result from hardening by precipitation of two semi-coherent phases, mostly the metastable D0<sub>22</sub>-Ni<sub>3</sub>Nb ( $\gamma''$ ) phase complemented with a small amount of L1<sub>2</sub>-fcc ( $\gamma'$  or Ni<sub>3</sub>Al) phase. This alloy contains Ni, Fe and Cr as main elements, Nb, Mo and Al as major additions but also in smaller quantities Ti, Co, C, Si, Mn, Ta, etc. The phases encountered during processing and service of Inconel 718 are the matrix fcc\_A1 ( $\gamma$ ), the stable D0<sub>a</sub>-Ni<sub>3</sub>Nb ( $\delta$  sometimes called also  $\beta$ ) and the metastable D0<sub>22</sub>-Ni<sub>3</sub>Nb ( $\gamma''$ ) and L1<sub>2</sub>-fcc ( $\gamma'$  or Ni<sub>3</sub>Al). In some occasions, other phases have been reported as MC and M<sub>6</sub>C carbides, Laves, and bcc\_A2 (Cr) and possibly  $\eta$  (hcp-Ni<sub>3</sub>Ti).

For simulating the phase transformations during processing and service, one needs to couple a thermodynamic software (Thermo-Calc [1]) with a diffusion one (DICTRA [1], or MICRESS [2]). We decided to focus on the quaternary Cr–Fe–Nb–Ni, and to build for it both a thermodynamic database and a mobility database. We present here our work on the ternary Fe–Nb–Ni.

Raghavan [3–5], (Fig. 1) has presented various short assessments and compilations of some references about the Fe–Nb–Ni system. The phases to take into account are liquid, fcc\_A1, bcc\_A2, C14\_Laves, D0<sub>a</sub>, D8<sub>5</sub> and L1<sub>2</sub>-fcc stable already on the binaries and

possibly C15\_Laves and C36\_Laves quoted by some authors [6–8]. Additionally, the metastable D0<sub>22</sub> phase is encountered experimentally [9–12].

The general idea of our study is, on one hand, to attempt to use ab-initio data for optimization work, in particular because we have to cope with metastable phases, and, on the other hand, to represent reasonably well the set of experimental data at different temperatures, with a minimum of parameters to be optimized, in order to build a quaternary database Cr–Fe–Nb–Ni as simply as possible. A bibliographic survey of the available optimizations for the limiting binary systems and of the ternary information will be first presented. Then ab-initio calculations performed as part of this work are detailed and compared to literature data. Finally a Calphad-type optimization, performed with TCCR (Thermo-Calc Classical version R) [1], is presented and illustrated.

We will use the assumption that the pressure dependence of the Gibbs energies can be neglected at a pressure about the atmospheric pressure  $p^\circ$ . Per default, the units in this publication are atomic or mole, percents or fractions for concentration, Joule for energies and Kelvin for temperatures.

## 2. Bibliographic survey

### 2.1. Unary and binary information

The unary Gibbs energies for the liquid fcc\_A1 and bcc\_A2 phases have been taken from the database SSOL2 [1]: they are from Dinsdale [13]. The unary Gibbs energies of formation of pure elements D0<sub>a</sub>, C14 and C15 set equal to 5000 J/mol-at. come from Dupin and Ansara [14] and Coelho et al. [15].

\* Corresponding author. Tel.: +33 5 62 88 56 75.

E-mail address: jacques.lacaze@ensiacet.fr (J. Lacaze).

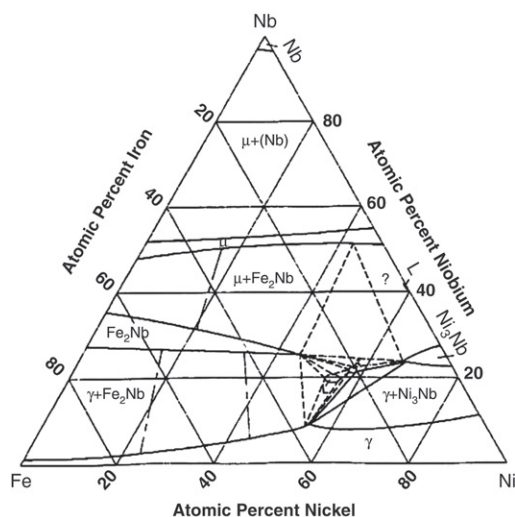


Fig. 1. Isothermal section of the Fe–Nb–Ni system at 1473 K from Takeyama et al. [8] reported by Raghavan [5].

We present here a short bibliographic study on previous estimations or optimizations of the Gibbs energies for the binary stable phases. The phases liquid, fcc\_A1, bcc\_A2 are phases commonly described with substitution on one sublattice for metallic elements, while the Laves phases C14, C15 and C36 are most of the time described with a two-sublattice model  $(A, B, C, \dots)_2(A, B, C, \dots)_1$  according to the Compound Energy Formalism (CEF). The models adopted for the other phases,  $DO_{10}$ ,  $D8_5$ ,  $DO_{22}$  and  $L1_2$  will be discussed below.

The magnetic properties of the phases have only been compiled by Dinsdale [13] for the unary fcc\_A1 and bcc\_A2, by Dinsdale and Chart [16] for Fe–Ni fcc\_A1 and by Bolcavage and Kattner [17] for Nb–Ni fcc\_A1. For fcc\_A1 in Fe–Nb and bcc\_A2 in all three binary systems, the magnetic properties, namely the second-order transition temperatures and the magnetic moments, were simply supposed to vary linearly between the values for pure elements. For the phases other than fcc\_A1 and bcc\_A2, the magnetic properties have neither been discussed nor described by any of the authors of Calphad-type assessments. As ab-initio calculations depend in particular on the starting assumption of the kind of magnetism (especially ferro or antiferromagnetism), a bibliographic study and a discussion about such magnetic properties are presented below for all the phases.

### 2.1.1. Fe–Nb

This binary presents, as stable phases, liquid, fcc\_A1, bcc\_A2, C14 and  $D8_5$  (Fig. 2).

The Fe–Nb available in the SSOL2 database is the one from Huang [18] where the C14 phase is stoichiometric and where the  $D8_5$  ( $\mu$ ) phase is described with a very narrow field of existence in composition and with a congruent melting, which is in disagreement with experimental data of Zelaya et al. [19].

Coelho et al. [15] proposed an optimization fitting correctly the experimental data and with a classical two-sublattice model for C14 and a model  $(Nb)_6(Fe, Nb)_7$  for  $D8_5$ .

The binary Fe–Nb has also been optimized by Srikanth and Petric [20] but with a stoichiometric  $D8_5$  not fitting the experimental data. Besides their C14 phase is treated with a three-sublattice model, not compatible with the two-sublattice one used by Costa et al. [21] for their optimization of Cr–Nb that we have selected for our work on the Cr–Nb–Ni and Cr–Fe–Nb systems [22].

The most recent assessment from Toffolon and Servant [23] was finally preferred to Coelho et al. [15]. In fact, Toffolon and

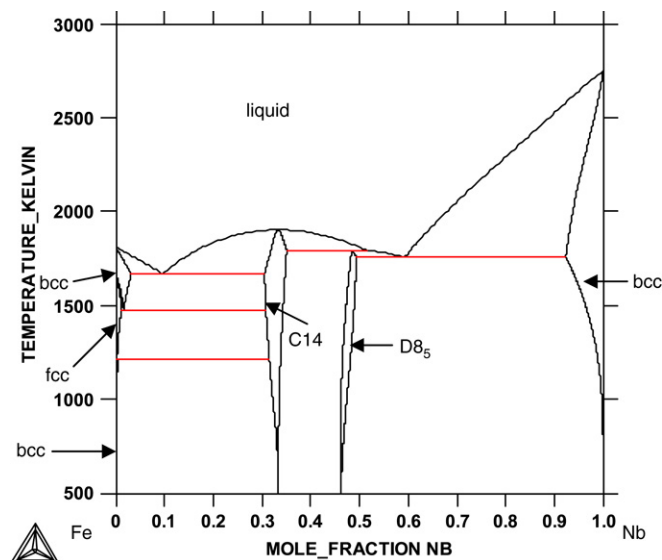


Fig. 2. Fe–Nb phase diagram calculated thanks to the optimization of Toffolon and Servant [23] (four sublattices for  $D8_5$ ).

Servant [23] published two optimizations with two different models for  $D8_5$  (a three- or a four-sublattice model).

In order to limit the number of parameters for this phase when extending the description to higher systems, it was decided to use a simple two sublattice model for  $D8_5$ . Therefore we had to re-adjust the parameters of the  $D8_5$  with a two-sublattice description.

None of the optimizations took into account any magnetic properties for the C14 phase or for the  $D8_5$  one.

Experimentally Read et al. [24] have studied the magnetic properties of  $Fe_2Nb$  (C14\_Laves) and of the  $D8_5$  phase by magnetic and Mössbauer measurements in the range 4–400 K. They conclude that  $D8_5$  is antiferromagnetic below 270 K and that the C14 is weakly ferromagnetic. In particular, they present the experimental evolution of its Curie temperature versus composition. Osipova and Panteleimonov [25] found that the  $Fe_2Nb$  intermetallic compound is paramagnetic at all temperatures but Shiga and Nakamura [26] found a composition dependent ferromagnetic behavior.

Inoue and Shimizu [27] have calculated the Density of States (DOS) for  $Fe_{2+x}Nb_{1-x}$  C14 by making use of Tight-Binding scheme and deduce properties of alloys based on the pair approximation as the Curie temperature and the corresponding ferromagnetic moment. They compared them to experimental values from Read et al. [24] and Shiga and Nakamura [26]. According to their calculation and to the data they quote, the properties are strongly dependent on the composition.

But other authors describe the  $Fe_2Nb$  C14 phase as a very weak anti-ferromagnetic phase. The Néel temperature was determined to be about 10 K [28,29] by magnetization measurements and Nuclear Magnetic Resonance (NMR), 21.4 K [30] by measuring the temperature dependence of hysteresis loops, initial Alternative Current (AC)-susceptibility and Zero Field Cooled-Field Cooled (ZFC-FC) magnetizations, or 18 K by Crook and Cywinski [31] thanks to Direct Current (DC) magnetization.

In fact, Crook and Cywinski [31] and Turtelli et al. [30] explain a more complicated magnetic behavior of the  $Fe_2Nb$  C14 with a ferro–antiferro magnetic competition depending on the temperature and on the composition.

For the bcc\_A2 phase, the linearity and the slope deduced from the unaries [13] is in good agreement with the ab-initio calculations for Fe-rich Fe–Nb bcc\_A2 alloys, performed by Kobayashi et al. [32] with the Koringa–Kohn–Rostoker Coherent

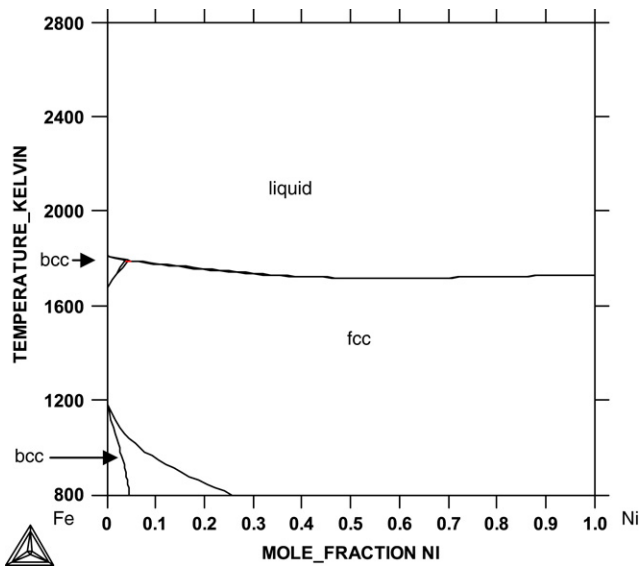


Fig. 3. Fe–Ni phase diagram calculated thanks to the optimization of Lee [35] (above 790 K).

Potential Approximation (KKR-CPA) based on the Local Spin Density Approximation (LSDA).

#### 2.1.2. Fe–Ni

The stable phases are liquid, fcc\_A1 and bcc\_A2 (Fig. 3) and additionally  $L1_2$ -fcc and  $L1_0$  at temperatures below 790 K.

Xing et al. [33], Gabriel et al. [34], Dinsdale and Chart [16] and Lee [35] have optimized Fe–Ni. But following Miettinen [36], the binary Fe–Ni we selected was taken from the database SSOL2 [1] (from [16]) and the modification proposed by Lee [35] for the liquid has been introduced, in order to be able to use the optimization of the ternary Cr–Fe–Ni from [36,37] for the quaternary system later on. It has to be noticed that the final aim of Lee's modification [35] was to better fit the Fe-rich composition properties, which is not our aim as we are interested in the Ni-rich side properties. But the modification does not lead to any lesser agreement of the rest of the diagram.

The modelling of the magnetic properties of fcc\_A1 is from SSOL2 [16].

Below 790 K, the ordered ( $Ni_3Fe$ )  $L1_2$ -fcc is stabilized. This part will be discussed later on (see 2.1.5). The  $L1_0$  phase (about 45% Fe–55% Ni) found stable at lower temperature (below about 590 K according to the calculation from Ohnuma et al. [38]) in Fe–Ni alloys from meteorites equilibrated for millions of years in space [39,40], has not been taken into account.

#### 2.1.3. Nb–Ni

This binary presents the phases liquid, fcc\_A1 and bcc\_A2,  $D0_a$  and  $D8_5$  (Fig. 4).

The optimization from Bolcavage and Kattner [17] with two-sublattice models for  $D0_a$  and for  $D8_5$  compatible with our other choices has been chosen and introduced. Other assessments by Kejun et al. [41], Chen and Du [42] and Joubert et al. [43] were rejected mainly because the  $D8_5$  ( $\mu$ ) was described with three, four or five sublattices.

It has to be noticed that Bolcavage and Kattner [17] took into account the composition dependence of the ferromagnetic Curie temperature of the Ni-rich fcc\_A1 solid solution determined by Ali-Zade et al. [44], with corresponding magnetic moment mixing parameters equal to 0, which means that the magnetic moment varies linearly with the composition.

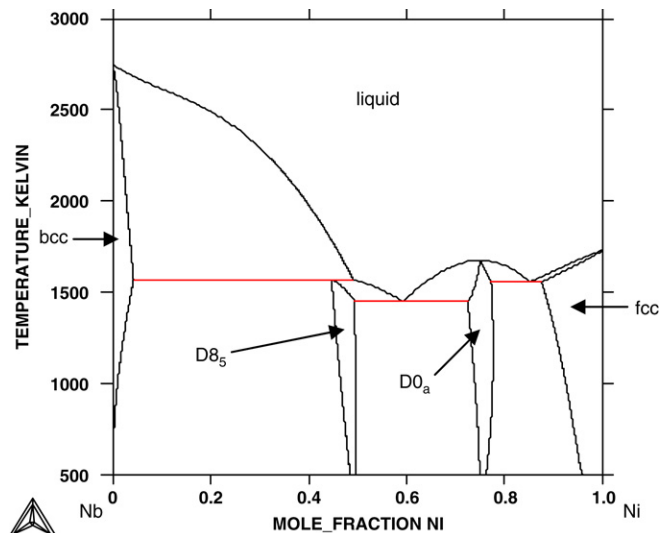


Fig. 4. Nb–Ni phase diagram calculated thanks to the optimization of Bolcavage and Kattner [17].

Osipova and Panteleimonov [25] found  $Ni_3Nb$  to be paramagnetic at all temperatures. Fangt et al. [45] investigated a single crystal of  $Ni_3Nb$   $D0_a$  (but with impurities, in particular, of Fe) with X-ray diffraction to determine the structure and with bulk magnetic measurements and neutron polarization analysis to characterize the enhanced paramagnetic behavior:  $D0_a$  is found to be paramagnetic, at least above 1.5 K, in agreement with [25].

Ravindran et al. [46] have investigated the physical properties of  $Ni_3Nb$   $D0_a$  non magnetic using the Tight-Binding Linear-Muffin Tin-Orbital Method (TBLMTO) within the Local-Density Approximation (LDA) and propose their heats of formation (referred to Ni fcc\_A1 and Nb bcc).

#### 2.1.4. The $D0_{22}$ phase

For this phase, magnetic determination, ab-initio results and optimized data are available only for the unaries.

In Inco718,  $D0_{22}$  is a tetragonal metastable phase formed on quenching and transforms to the stable orthorhombic  $D0_a$ . There are many structures related to  $D0_{22}$  and the continuity between different lattices depends on the tetragonal  $c/a$  ratio [47], which has caused some confusion of names used for such lattices in some publications. This led us to also investigate data for the body centered tetragonal (bct) structure as it is closely related to the  $D0_{22}$  structure.

It has to be pointed out that some of the data of the literature are for thin layers and not for bulk.

Mitsuoka et al. [48] have evaluated the magnetic moment of Fe bct from magnetization and Mossbauer spectra measurements for the Fe–C, Fe–N and Fe–Ni–C systems. They estimate it to vary from 2.2 to 2.6  $\mu_B$ /at. depending on the  $c/a$  ratio.

Kattner and Boettinger [49] have optimized the ternary system Ti–Al–Nb where this phase is stable based on the stable  $Al_3Nb$  and  $Al_3Ti$   $D0_{22}$  and for that in particular the  $\Delta G^{\text{form}}$  of Nb  $D0_{22}$  (reference liquid). We made the modification to refer it to Nb bcc\_A2 and we obtained a  $\Delta H^{\text{form}}$  ( $Nb_4$ , 0 K) = 87126.2 J/mol (or 88000 J/mol. using their own Gibbs energies). It can be compared with the value obtained for pure Vanadium  $D0_{22}$  proposed by Watson and Hayes [50]:  $\Delta H^{\text{form}}$  ( $V_4$ , 0 K) = 32000 J/mol. It has to be noticed that Watson and Hayes [50] do not specify the structure of their  $Ni_3V$  phase but it is well-known that, in the Ni–V binary system, the disordered fcc\_A1 solid solution 75% Ni–25% V transforms below about 1318 K [51,52] to form an ordered bct



phase [47] and more precisely a  $D0_{22}$  as confirmed by X-ray diffraction in the most recent studies like for instance [53–55]. In both cases [49] and [50], the  $D0_{22}$  is modelled with a two-sublattice model  $(A, B, C)_1(A, B, C)_3$ .

Kamada et al. [56] have experimentally evaluated the magnetic moment of Ni bct on a bcc-Fe(001) layer to be  $0.8 \mu_B$  at 4.5 K where they assume that the moment of Fe is equivalent to that of bulk Fe. Zhu et al. [57] have conducted a systematic ab-initio study on the Curie temperature as a function of the tetragonal distortion ( $c/a$ ) i.e. the gradual transformation from Ni bcc\_A2 ( $c/a = 1$ ) to Ni fcc\_A1 ( $c/a = 1.414$ ), using the Linearized Augmented Plane-Wave (LAPW) method in the Local Spin-Density Approximation (LSDA) together with the Monte-Carlo (MC) simulations. They have calculated the Curie Temperature,  $T_C$ , of Ni  $D0_{22}$  to increase of some 180 K from the  $T_C$ (Ni bcc) to  $T_C$ (Ni fcc) with the  $c/a$  ratio. But their  $T_C$ (Ni bcc) and  $T_C$ (Ni fcc) Curie temperature are significantly lower than those in the SSOL2 database where the difference is besides only 58 K.

Zhang et al. [58] have investigated the structural stability and theoretical strength of fcc\_A1 crystals under uniaxial loading by combining the Modified Analytical Embedded Atom Method (MAEAM) with the Modified Born Stability criteria. From their energies of formation of Ni bct and Ni fcc\_A1, we can deduce the  $\Delta H^{\text{form.}}$  (0 K) of Ni bct referred to Ni fcc\_A1. Nothing about magnetism is specified in the publication.

Watson and Hayes [50] has optimized the Ni–V system and proposes the Gibbs energy of formation of  $Ni_4 D0_{22}$ . His  $\Delta H^{\text{form.}}$  ( $Ni_4$ ,  $T = 0$  K) is 5 times lower than the one deduced from the ab-initio calculations [58].

### 2.1.5. The $L1_2$ -fcc phase

The  $L1_2$ -fcc  $\leftrightarrow$  fcc\_A1 transformation is an order–disorder transition and has to be modelled as such [59,60]. This means that the Gibbs energies of the pure elements Cr, Fe, Nb and Ni in the  $L1_2$ -fcc ordered phase are equal to the fcc\_A1 ones. It is possible to introduce a specific magnetism for  $L1_2$  by adding to the magnetic properties (transition temperature and magnetic moment) of fcc\_A1 additive ordered terms [61]. This can be done only for the case when there are enough data for the fitting.

For this phase we found only data for the Fe–Ni and the Nb–Ni systems.

As part of their optimization of the Cu–Fe–Ni system Servant et al. [62] have proposed a Gibbs energy description of the Fe–Ni  $L1_2$  phase, taken from an unpublished work by Ansara [63]. Ansara [63] used the two-sublattice model (interstitial site not counted) but Servant et al. [62] converted it to four sublattices. We translated it “back” to a two-sublattice model thanks to conversion formula [65,62,66]. The four-sublattice model is considered more general than the two-sublattice one but, again, the purpose here is to be able to use a simple enough model. The Fe–Ni phase diagram including  $L1_2$  is presented on Fig. 5.

It seems appropriate to investigate the literature on magnetic properties and ab-initio calculations in order to have a point of comparison and evaluation of the validity of our model and choice.

Himuro et al. [67] investigated the order–disorder and the Curie temperatures of  $FeNi_3$ – $Ni_3Si$  and  $FeNi_3$ – $AlNi_3$  by means of metallographic observation, Electron Probe Micro-Analysis (EPMA), Differential Scanning Calorimetry (DSC), electrical resistivity and vibrating sample magnetometry. From their experimental results, they deduced by extrapolation the Curie temperature for the ordered  $L1_2$ - $FeNi_3$  to be 953 K; they point out that they are in agreement with the value of 954 K from Wakelin and Yates [68]. It has to be noticed that the  $T_C$ (fcc\_A1,  $FeNi_3$ ) calculated from [16] chosen for our thermodynamic database is 888.4 K. Similarly, Ohnuma et al. [38] pointed out that the magnetic moment of the  $FeNi_3 L1_2$  is slightly higher than the one of fcc\_A1 for the same composition.

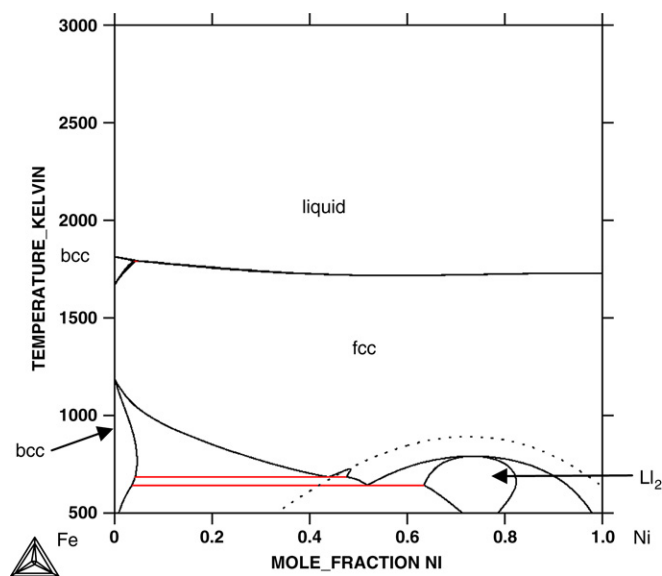


Fig. 5. Fe–Ni phase diagram calculated thanks to the optimizations of Lee [35] and of Servant et al. [62]. The Curie temperature is the dotted line.

Mischin et al. [69] have investigated first-principles calculations of the energy of  $FeNi_3$  and  $Fe_3Ni L1_2$  (reference Fe bcc\_A2 and Ni fcc\_A1), using the Spin-Polarized Linearized Augmented-Plane-Wave (LAPW) within the Generalized Gradient Approximation (GGA) method. They treated the  $L1_2Fe_3Ni$  compound as ferromagnetic. Their value for  $FeNi_3 L1_2$  is in good agreement with the optimized ones by Ansara [63]. But their energy of formation calculated for  $Fe_3Ni$  is drastically different from the one optimized by Ansara [63] (and with opposite signs).

Lechermann et al. [70] have investigated the physical properties of the ternary intermetallic system Ni–Fe–Al by combining ab-initio electron theory and statistical mechanics. They obtained in particular the energies of formation for  $Ni_3Fe$  and  $Fe_3Ni L1_2$  referred to Fe bcc\_A2 (ferromagnetic) and Ni fcc\_A1 (ferromagnetic) under the hypothesis of ferromagnetism and of no magnetism. Their energies of formation at 0 K of  $Ni_3Fe L1_2$  fit with [69,63].

Chen et al. [71] have performed ab-initio calculations on Fe–Ni  $L1_2$  alloys by combining the Full Potential Linearized Augmented-Plane-Wave (FLAPW) within the Generalized Gradient Approximation (GGA) method and the Cluster Variation Method (CVM) through the Cluster Expansion Method. Their curves obtained by spin-polarized calculation give the formation energy (reference Fe bcc\_A2 and Ni fcc\_A1) versus the lattice parameter. From them, we can deduce (for the minimum of energy) the  $\Delta H^{\text{form.}}$  (0 K) of  $Fe_3Ni$  and  $FeNi_3 L1_2$  (and the corresponding lattice parameter) under the assumption of ferromagnetism. The authors remark that magnetism has a crucial role on the phase stability of the Fe–Ni system. Their values are in good agreement with the ones from [69].

Ravindran et al. [46] have investigated the physical properties of  $Ni_3Nb L1_2$  (and  $D0_a$ ) using the Tight-Binding Linear-Muffin Tin-Orbital method (TBLMTO) within the Local-Density Approximation (LDA) and propose the corresponding heats of formation (reference Ni fcc\_A1 and Nb bcc\_A2).

Huang et al. [72] have studied the phase stability of  $Ni_3Nb$  and  $Nb_3Ni L1_2$  by using the Linearized-Muffin Tin-Orbital method with the Atomic Sphere Approximation (LMTO-ASA). They propose the energies of formation of these two metastable compounds (reference fcc\_A1 for Ni and bcc\_A2 for Nb). Their result for  $Ni_3Nb L1_2$  is close but slightly lower than the energy of formation obtained by [46].

Du et al. [73] have optimized the Al–Nb–Ni ternary system and propose parameters for the metastable Nb–Ni  $L1_2$  phase. It has to be noticed that their enthalpy of formation of  $Ni_3Nb$  (the stable composition) is half the ab-initio one from [46] but only a third of the value from [72]. The enthalpy of formation of the  $Nb_3Ni$   $L1_2$  compound was set equal to that of the  $Ni_3Nb$   $L1_2$  by Du et al. [73] which is only half of the value according to Huang et al. [72].

## 2.2. Ternary information

### 2.2.1. Experimental data

Available experimental data are exclusively of the phase diagram but few are really useful for optimizing the stable phase diagram. They are from [6–12,74–79]. Most of the samples experimentally investigated were first arc-melted and quenched. Then they were held at different temperatures and times to obtain equilibrium and finally quenched again.

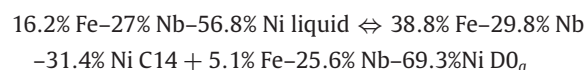
For the alloy 67.3% Fe–3.1% Nb–29.6% Ni, Manenc et al. [9], Kirman [10] and Manenc [11] agree on the formation of a metastable  $DO_{22}$  at a temperature about 873 K.

Peard and Borland [74] noted also the presence of the orthorhombic  $DO_a$  (Fe, Ni) $_3Nb$  and of Laves phases  $Fe_2Nb$  formed after ageing various time at 1048 K for the alloy 56.4% Fe–3.8% Nb–39.8% Ni.

Leitch and Chaturvedi [75] have studied the precipitation reactions in five alloys about 67%–70% Fe–3%–1% Nb–30%–29% Ni, homogenized 75 h at 1523 K, aged or not at 1073 K. By measuring the variation in hardness and lattice parameter versus Nb concentration, they could deduce the limit of solubility of Nb in fcc\_A1 to be about 2.1% in Nb (for 68.5% Fe–29.4% Ni) at 1523 K but only of 0.6% (for 70.3% Fe–29.1% Ni) at 1073 K.

Quist et al. [12] have studied the influence of Fe on the precipitation of metastable  $DO_{22}$  in the system Fe–Nb–Ni. The metastable  $DO_{22}$  does not appear in the binary Nb–Ni alloys but the introduction of Fe promotes it. In particular, they studied four alloys, 1% Fe–10% Nb–89% Ni (Alloy 1), 3% Fe–10% Nb–87% Ni (Alloy 2), 1% Fe–12.5% Nb–86.5% Ni (Alloy 3) and 3% Fe–12.5% Nb–84.5% Ni (Alloy 4), with impurities of Al, Ti and C (less than 0.06%). Alloys 1 and 2 were treated at 1523 K. The alloys 3 and 4 were held at 1553 K during 30 min, quenched and then aged between 523 and 1273 K for times up to 200 h. For the alloys 1, 2 and 3, they found no precipitation of  $L1_2$  nor  $DO_{22}$ . But for their alloy 4, the precipitation of  $DO_{22}$  occurs during aging at 773 K.

Panteleimonov and Aleshina [76] have studied Fe–Nb–Ni alloys annealed at 1173 K during 1800 h on the pseudo binary  $Fe_2Nb$ – $Ni_3Nb$ , by X-ray Diffraction (XRD), Scanning Electron Microscopy (SEM) and microhardness, Differential Thermal Analysis (DTA). They found a pseudo-binary eutectic equilibrium at  $T = 1563$  K:



Varli et al. [77] studied by X-Ray diffraction (XRD) samples of Fe–Nb–Ni alloys aged 600 h at 1223 K and noticed that the  $D8_5$  phase is continuous across the ternary from  $Nb_5Fe_7$  to  $Nb_6Ni_7$  and that the maximum of solubility of Ni in  $Fe_2Nb$  C14 is at 47% Fe–33% Nb–20% Ni.

Skakov et al. [78] studied the effect of the cooling rate of many alloys from the liquid down to 298 K. Although their results, made by fast quenching of very small amounts, cannot furnish us with any useful quantitative data, they point out the influence of the treatment (and of the size of the sample) on the phases formed. In particular, with a very fast cooling speed, a solid amorphous phase and a  $D8_5$  phase, distorted or not, seem to be formed preferentially to the stable C14 and  $DO_a$ .

Savin [6] has studied samples of Fe–Nb–Ni quenched from the liquid state. The author measured, for different quenching rates, by X-Ray diffraction (XRD) and Scanning Electron Microscopy coupled with an Energy Dispersive X-ray Detection (SEM-EDX), the phases present and their compositions. At the highest rates, amorphous state and phases as C15 or distorted  $D8_5$  appear. They note a C36 for the composition 40% Fe–40% Ni–20% Nb even at their lowest quench rate, that is anyway very high (100–1000 K/s). By comparing their experimental data in the binary systems with the established binary phase diagrams, they conclude their experiments obtained for the lowest rate of cooling in the ternary system to be representative of the stable state at 1273 K. But in their ternary isothermal section at 1273 K they keep inconsistently C15 as a stable phase appearing in the middle of the ternary. It seems reasonable to take only into account their results obtained for the lowest rate of quenching and therefore to treat C15 as metastable.

Ueyama et al. [79] have studied the 10% Fe–15% Nb–75% Ni alloy equilibrated 240 h at 1473 K and then water quenched. They have determined the composition of the phases in equilibrium by Electron Probe Micro-Analyzer analysis (EPMA) and they identified the phases by powder X-Ray Diffraction (XRD):  $DO_a$  and fcc\_A1.

Takeyama et al. [7] have determined for seven Fe–Nb–Ni alloys, (5% Fe–15% Nb–80% Ni, 10% Fe–15% Nb–75% Ni, 15% Fe–15% Nb–70% Ni, 25% Fe–15% Nb–60% Ni, 5% Fe–25% Nb–70% Ni, 15% Fe–25% Nb–60% Ni and 25% Fe–20% Nb–55% Ni), homogenized 24 h at 1523 K and then treated 240 h at 1473 K, the phases in equilibrium by powder X-Ray Diffraction (XRD) and Transmission Electron Microscope (TEM). The composition of the phases were analyzed by Electron Probe Micro-Analyzer (EPMA). They found for the sample 25% Fe–15% Nb–60% Ni an unknown phase identified to be an  $A_3B$ -type ordered hexagonal  $hP24$  phase that they localized for the composition 20% Fe–22% Nb–58% Ni. It has to be noticed that the “ $A_3B$ -type” does not correspond to a C36 Laves phase but it seems that the  $A_3B$ -type was a typographical error and that it should have been more likely an “ $A_2B$ -type”.

In this case, Savin [6] and Takeyama et al. [7] do not agree about the composition of the possible C36 phase. Indeed, it seems unlikely that the C36 could have a composition field of existence so large (20%–40% Fe–22%–20% Nb–58%–40% Ni) or such a drastic change from 1273 K at 40% Fe–20% Nb–40% Ni–20% Fe–22% Nb–58% Ni at 1473 K.

Takeyama et al. [8] have determined for four Fe–Nb–Ni alloys, (65% Fe–15% Nb–20% Ni, 45% Fe–15% Nb–40% Ni, 15% Fe–25% Nb–60% Ni and 46.7% Fe–33.3% Nb–20% Ni), the composition of the phases in equilibrium at 1473 K, on samples equilibrated 240 h at 1473 K, by Electron Probe Micro-Analyzer measurements (EPMA). Phase identification was done by powder X-Ray Diffraction (XRD).

### 2.2.2. Ab-initio data

For  $NbFe_2$  C14, paramagnetic according to Osipova et Panteleimonov [25], Asano and Ishida [80] studied the electronic structure of both  $NbCr_2$  and  $NbFe_2$  in both C14 and C15 structures, by ab-initio calculation using the Linear Muffin-Tin Orbital (LMTO) method within the framework of the Local Spin Density (LSD) approximation. They propose the energy of formation of C15 from C14 for the non-magnetic state. From the optimized enthalpy of formation at 0 K of  $NbFe_2$  C14 (–73200 J/mol) [23] and from [80], an estimation for the enthalpy of formation of the  $NbFe_2$  C15 can be deduced: –67686.5 J/mol.

### 2.2.3. Estimation and optimizations

Miettinen [81] has proposed interaction parameters for the Fe-rich liquid, bcc\_A2 and fcc\_A1 phases where the solute contents are very small. He estimated the liquid one to be equal to the one evaluated for Cr–Fe–Nb [81] (+40000 J/mol) and the bcc\_A2 and fcc\_A1 ones to be 0. It should only be considered as a first approximation to be tested.

This ternary has been already optimized by Saunders and Miodownik [82] for the encrypted database TTNI6 [1] and by Valdes et al. [83], but in this latter case, the results are not yet published. It seems that Valdes et al. [83] reproduce well the ternary data from Takeyama et al. [7] at 1473 K but contrary to TTNI6, they chose for the binary Fe–Nb a narrow composition range for C14 like Toffolon and Servant [23] and in this publication. It seems inconsistent to ignore the wide binary composition range of C14 at 1473 K obtained experimentally by Takeyama et al. [8] but to fit the same wide range in the ternary.

## 2.3. Modelling and possible assumptions

### 2.3.1. Modelling

Table 1 lists for each phase involved in the ternary Fe–Nb–Ni system:

- the phase name used in this publication, the name used in our ternary thermodynamic database (TDB) and other possible names found in the literature,
- the crystallographic information according to [47],
- the systems where the phase is stable.

The Redlich–Kister–Muggianu formalism of the substitutional model and the compound energy formalism (CEF) have been used systematically.

The question mark “?” that can be found in the table means simply that experimental works disagree about the stability of the phase in the studied system and that we decided in our optimization to consider these phases (C15 and C36) as not stable.

For all formula describing a phase Gibbs energy in function of the temperature and of the composition, magnetism included, see the Appendix A.

### 2.3.2. Possible assumptions

**2.3.2.1. Reciprocal constraints for two-sublattice CEF modelled phases.** Considering a stable intermetallic compounds  $A_xB_y$ , the reciprocal constraints (called also by abuse of the language Wagner–Schottky constraints [84]) link the Gibbs energy of an antistructure  $B_xA_y$  compound with those of  $A_xA_y$ ,  $B_xB_y$  and  $A_xB_y$ . As long as the composition range is enough narrow, it is a very practical method to estimate the CEF parameter of the antistructure  $B_xA_y$ . Wagner–Schottky intended their model to be restricted to “dilute solutions of defects” i.e. small values of the site fractions  $y^{\text{sublat},1}(B)$  and  $y^{\text{sublat},2}(A)$ , whereas the CEF modelling extends across the whole system (see Appendix A).

The reciprocal constraints have been introduced in particular by Costa et al. [21] – for their Cr–Nb optimization we chose for our Cr–Fe–Nb and Cr–Nb–Ni optimizations [22] –, by Toffolon and Servant [23] and Bolcavage and Kattner [17], for the Gibbs Energy of the C14, C15 or  $D0_a$  intermetallic compounds  $B_xA_y$  containing antistructure atoms relative to the stable  $A_xB_y$ . These constraints can be introduced for the entire ternary description of the C14, C15 (and C36) Laves phases and of the  $D0_a$  phase, so that: for a phase  $\phi$  ( $\phi = \text{C14, C15, C36 or } D0_a$ ) modelled as  $(A, B)_x(A, B)_y$ , with  $A \neq B$  and  $A$  or  $B = \text{Fe, Nb or Ni}$  and with  $(x, y) = (2, 1)$  for C14, C15 and C36 or  $(x, y) = (1, 3)$  for  $D0_a$ :

$$\Delta G(\phi, B:A) = \Delta G(\phi, A:A) + \Delta G(\phi, B:B) - \Delta G(\phi, A:B).$$

Watson and Hayes [50] have made an optimization of the Ni–V system where the  $D0_{22}$  has been modelled with the same reciprocal constraints:

$$\Delta G(D0_{22}, \text{Ni:V}) = \Delta G(D0_{22}, \text{V:V}) + \Delta G(D0_{22}, \text{Ni:Ni}) - \Delta G(D0_{22}, \text{V:Ni}).$$

**2.3.2.2. The  $L1_2$  phase.** For the  $L1_2$ -fcc phase, constraints are derived from the fact that  $L1_2$  must disorder to a fcc\_A1 phase with the same fraction for each constituent on all its sublattices. These constraints for the  $L1_2$   $(A, B, C)_{0.75}(A, B, C)_{0.25}$  two-sublattice model can be implemented in different ways [59]. We mainly found assumptions like in the works from Dupin et al. [66] for Cr–Ni and from Du et al. [73] for Nb–Ni:

- the hypothesis  $\Delta G(L1_2, A:B) = \Delta G(L1_2, B:A)$
- with or without  $L(L1_2, A, B:B) = L(L1_2, A, B:A)$
- with or without  $L(L1_2, A, B:A \text{ or } B) = 2 * \Delta G(L1_2, A:B) [= 2 * \Delta G(L1_2, B:A)]$
- with or without  $L(L1_2, A, B:*) \neq 0$  but  $L(L1_2, *:A, B) = 0$ .

It has to be noticed that none of these approximations is followed by [63,62] for Fe–Ni.

When extrapolating to higher systems, it is necessary to check that in the disordered fcc\_A1, the same fraction on both sublattices for each constituent is calculated. To ensure this, corrective terms for ternary interaction parameters may have to be introduced [59,86].

**2.3.2.3. Other estimations used.** For the phases C14, C15,  $D0_a$ , and  $D0_{22}$ , several assumptions have been more or less systematically introduced as possible starting estimations:

- A:B is like C:B if A and C are Fe or Ni and A:B is like A:C if B and C are Fe or Ni,
- A:Nb may be like A:V
- A, B:C = 0 and C:A, B = 0 if A and B are Fe, or Ni
- A, Nb:C = A, Nb:B and C:A, Nb = B:A, Nb
- A, Nb:C = B, Nb:C and C:A, Nb = C:B, Nb.

In the optimization procedure, these initial assumptions will be kept if they prove to be good enough or if, on the other hand, they have no impact on the calculation (see Appendix B).

## 3. Ab-initio calculations

In the following we use AI for ab-initio, TDB for our database, AFM for antiferromagnetic, FM for ferromagnetic, NFM for non ferromagnetic (that means calculated non magnetic but under the hypothesis of a possible ferromagnetism), NM for non magnetic PM for paramagnetic. It has to be noticed that AI-calculations under the hypothesis of NM or under the hypothesis of FM do not lead necessarily to the same energy nor the same lattice constant even if the compound is calculated NFM.

### 3.1. Method

The lack of experimental data led us to estimate parameters using the enthalpies of formation at 0 K,  $\Delta H^{\text{form.}}(T = 0 \text{ K})$ , deduced from ab-initio (first-principles) simulations.

Therefore, the energies of Fe and Nb bcc\_A2 and Fe, Nb and Ni fcc\_A1 and of all the CEF compounds for the phases C14, C15,  $D0_a$ ,  $L1_2$  and  $D0_{22}$  have been calculated according to the Density Functional Theory (DFT) under the hypothesis of ferromagnetic effect and/or of non-magnetic effect.

In all cases, the approximation used is the Perdew–Burke–Ernzerhof Generalized Gradient Approximation (PBE-GGA) within its spin version [87] combined with the Projected Augmented



**Table 1**  
Names of each phase involved in this study, its crystal structure, the systems where the phase is experimentally found stable, and the models.

Names	Name used in the publication	Common name in publications	Crystallographic information				Stability			Modelling	
			Designation Strukturbericht	Prototype	Space group classes	Pearson symbol	Space group	Unaries	Binaries	Ternary Fe–Nb–Ni	Modellisation in sublattices
Liquid	L1QUID	(L)						Fe Nb	Fe–Nb Fe–Ni	Stable	(Fe, Nb, Ni) <sub>1</sub>
bcc_A2	BCC_A2	( $\alpha$ ) or ferrite	A2	W	Cubic	cI2	Im $\bar{3}$ m	Ni Fe Nb	Nb–Ni Fe–Nb Fe–Ni	Stable	(Fe, Nb, Ni) <sub>1</sub> (Va) <sub>1</sub>
fcc_A1	FCC_A1	( $\gamma$ ) or austenite	A1	Cu	Cubic	cF4	Fm $\bar{3}$ m	Fe	Fe–Nb Fe–Ni	Stable	(Fe, Nb, Ni) <sub>1</sub> (Va) <sub>1</sub>
D8 <sub>5</sub>	D85_Ni7Nb6	( $\mu$ )	D8 <sub>5</sub>	Fe <sub>7</sub> W <sub>6</sub>	Trigonal	hR13	R $\bar{3}$ m	Ni None	Nb–Ni Fe–Nb	Stable	(Nb) <sub>6</sub> (Fe, Nb, Ni) <sub>7</sub>
D0 <sub>a</sub>	DOa_Ni3Nb	( $\delta$ , or sometimes $\beta$ or even $\rho$ )	D0 <sub>a</sub>	$\beta$ -Cu <sub>3</sub> Ti	Orthorhombic	oP8	Pmmn	None	Nb–Ni	Stable	(Fe, Nb, Ni) <sub>1</sub> (Fe, Nb, Ni) <sub>3</sub>
C14	C14_LAVES	( $\epsilon$ ) or ( $\lambda_1$ )	C14	MgZn <sub>2</sub>	Hexagonal	hP12	P6 <sub>3</sub> /mmc	None	Fe–Nb	Stable	(Fe, Nb, Ni) <sub>2</sub> (Fe, Nb, Ni) <sub>1</sub>
C15 ?	C15_LAVES	( $\beta$ ) or ( $\lambda_2$ )	C15	Cu <sub>2</sub> Mg	Cubic	cF24	Fd $\bar{3}$ m	None	None	Metastable	(Fe, Nb, Ni) <sub>2</sub> (Fe, Nb, Ni) <sub>1</sub>
C36 ?	C36_LAVES	( $\lambda_3$ )	C36	MgNi <sub>2</sub>	Hexagonal	hP24	P6 <sub>3</sub> /mmc	None	None	Supposed none	(Fe, Nb, Ni) <sub>2</sub> (Fe, Nb, Ni) <sub>1</sub>
D0 <sub>22</sub>	D022_Ni3Nb	( $\gamma''$ )	D0 <sub>22</sub>	Al <sub>3</sub> Ti	Tetragonal	tI8	I4/mmm	None	None	Metastable	(Fe, Nb, Ni) <sub>1</sub> (Fe, Nb, Ni) <sub>3</sub>
L1 <sub>2</sub>	L12_FCC	$\gamma'$ or Ni <sub>3</sub> Al	L1 <sub>2</sub>	Cu <sub>3</sub> Au	Ordered fcc	cP4	Pm $\bar{3}$ m	None	Fe–Ni	Stable	(Fe, Nb, Ni) <sub>0.75</sub> (Fe, Nb, Ni) <sub>0.25</sub> (Va) <sub>1</sub>

Wave (PAW) pseudopotential approach. Most of the comparable works found in the literature are based on another approximation: the Local Density one (LDA). But the GGA approximation is considered to be better than the LDA approximation for most metallic compounds.

This work has been performed using a computational implementation program of the Density Functional Theory, the Vienna Ab-Initio Simulation Package [88–91] combined with the corresponding database from Kresse and Joubert [92]. A 400 eV energy cut-off has been used for structure optimizations and increased up to 500 eV for the formation energies. The uncertainty of our ab-initio calculations due to the imprecision in the convergence is about 3–5 meV/at., that is to say about 0.3–0.5 kJ/at.

From these energies at 0 K obtained under the hypothesis of a possible FM state, we deduced first the energies of formation of all the CEF compounds (FM or NFM) of C14, C15, D0<sub>a</sub> and D0<sub>22</sub> referred to the bcc\_A2 phase for Fe (FM) and Nb (NFM) and to the fcc\_A1 phase for Ni (FM). In these three cases of Fe bcc\_A2 FM, Nb bcc\_A2 NFM and Ni fcc\_A1 FM, AI assumptions are in agreement with experimental data and our TDB.

We calculate also the energies of formation of D0<sub>a</sub> CEF compounds under the hypothesis of NM and referred to the same as above. Then we added to them, the magnetic enthalpy effect of magnetism of Fe bcc\_A2 FM and Ni fcc\_A1 FM using the AI magnetic moment, the Curie temperatures already TDB-optimized and stored in the SSOL2 database and the formula developed in Appendix A. Indeed, the enthalpies (and generally the Gibbs energies) of formation entered in a database according to the SGTE formalism are referred to the elements in one of their stable (or unstable) phase without any magnetic effect:

$$\begin{aligned} G(\phi, A_x B_y) &= A + BT + CT \ln T + \dots + xG_A^\alpha + yG_B^\beta \\ &= \Delta G^{\text{form.}}(\phi, A_x B_y) + xG_A^\alpha + yG_B^\beta \end{aligned}$$

with  $G_A^\alpha$  and  $G_B^\beta$  most of the time equal to the functions GHSERA and GHSEB (but not always), see Appendices A and B.

In the case of the energies of formation of all the CEF compounds of L1<sub>2</sub>, we referred them to the fcc\_A1 phase for Fe (AI-calculated under the hypothesis of NM but experimentally and TDB-optimized AFM), for Nb (NFM) and for Ni (FM). AI assumptions are in agreement with experimental data and our TDB only for Nb fcc\_A1 NFM and Ni fcc\_A1 FM.

It has to be noticed that whatever is the available ab-initio method, the proposed parameter is an energy of formation at 0 K. Therefore, under certain conditions, it is possible to discuss it and enter it as an enthalpy of formation (at 0 K), and under the assumption of the Kopp–Newman rule (no parameter for the heat capacity of formation) as an enthalpy of formation at any temperature.

## 3.2. Results and discussion

### 3.2.1. General remarks

There are several restrictions in comparing the optimized or estimated coefficient A of our TDB (or the other used A of the literature) and the ab-initio  $\Delta H$  under the hypothesis FM (or NFM) or NM.

First, our different phases, except the L1<sub>2</sub>, can only be described in an optimization as NM due to the lack of data (on the real type of magnetism AFM or FM, on the AFM magnetic moment  $\beta$  if it is AFM and systematically on the corresponding Curie or Néel temperature). Besides, even in the case of the L1<sub>2</sub>, again due to the lack of data, our database follows the approximation that the magnetic moment  $\beta$  and the corresponding magnetic transition temperature of L1<sub>2</sub> is equal to the fcc\_A1 ones, which means that

the solution is calculated in the database as AFM or FM depending on the composition.

In most cases we know little or nothing about the kind of magnetism of the CEF compounds, especially of the “metastable” ones and besides, our ab-initio calculations as the ones of the literature, have been made only for a possible FM (or NM).

Secondly, Fe fcc is AFM in our TDB, while as explained below, we used the AI Fe fcc NM for referring the AI enthalpies of formation of some of the L1<sub>2</sub> CEF compounds: the difference is −0.25 kJ/mol. Besides even for Ni fcc and Fe bcc for which we introduced the corrections of the purely magnetic effect to the AI enthalpy at 0 K, the differences between the TDB magnetic moments and the AI ones induce supplementary discrepancies. For Ni fcc, the difference between the TDB purely magnetic enthalpy at 0 K and the AI one is +0.28 kJ/mol. For Fe bcc, the corresponding difference is −0.05 kJ/mol.

Thirdly, when the  $\Delta G^{\text{form.}}(\phi, A_x B_y)$  entered in our TDB is independent of temperature, i.e. reduced to the coefficient A, the order of magnitude of A is in fact an average of the  $\Delta H^{\text{form.}} - T\Delta S^{\text{form.}}$  expression for T belonging to the studied range (more or less 500–1500 K), which means that an A different from an AI energy does not mean necessarily that there is disagreement between both. Besides, the field of validity of all formula in the TDB is for  $298 \leq T \leq 3000$  K. Anyway, we extrapolated it until 0 K in particular as in our case for the elements A or B = Fe or Ni and  $\phi$  = bcc or fcc:

$$\Delta H^{\text{TDB only magn.}}(\phi, A_x B_y, 298 \text{ K}) \approx \Delta H^{\text{TDB only magn.}}(\phi, A_x B_y, 0 \text{ K}).$$

Fourthly, a CEF compound energy of formation (for A<sub>x+y</sub> or A<sub>x</sub>B<sub>y</sub>) contributes to the total Gibbs energy of the phase proportionally to the fraction of the CEF compound. That means that some CEF compounds (and especially of course the ones that are stable) are more important than others to have a good description of the total Gibbs energy. A disagreement between the AI energy of formation and the chosen enthalpic A of a A<sub>x+y</sub> or A<sub>x</sub>B<sub>y</sub> compound far away from the stoichiometry of the stable composition is not so important in the modelization for optimization.

Fifthly, for the A<sub>x+y</sub> CEF compounds of the D0<sub>a</sub> and C14 or C15 Laves phases, the previous optimizations had been done using a Gibbs energy of formation independent of the temperature (and also of the element A): simply equal to 5000 J/mol of atoms [14, 15]. Therefore it is impossible to modify them and test the ab-initio calculations without modifying (re-optimizing) the binaries, a task that was not our purpose.

### 3.2.2. Comparison

Wang et al. [93] propose a systematic first-principles calculation for the total energies of 78 pure elemental solids (bcc\_A2 fcc\_A1 and hcp\_A3) at 0 K using the projector augmented wave method (PAW) within the generalized gradient approximation and the Perdew–Wang parameterization (GGA-PW91) [94]. They deduce and compare the energies of formation of these 78 elements fcc (and hcp) referred bcc, to the corresponding enthalpies of formation at 298 K from the SGTE SSOL2 [1] (and from the Saunders’ databank [95]). The study is very interesting but they compare data under different conditions: for instance Fe is AFM in the SSOL2 [1] database as it is the case experimentally, while they seem to have performed the calculation under the hypothesis of FM (or maybe NM) for all elements. Their results for the energies of formation of Nb and Ni fcc referred to bcc are in good agreement with ours (less than 3% of difference). For Nb fcc referred to Nb bcc, the disagreement between [95] and their results is less (+29.5%) than the disagreement between SSOL2 [1] and their results (+56%) but still significant. For Ni fcc referred to Ni bcc, the agreement is better: respectively +13% to +18%. But our enthalpy of formation at 0 K of Fe fcc referred to bcc (both FM) is 78% higher than their value

(15.1 kJ/mol and 8.45 kJ/mol respectively) and their value is a better fit with the one from SSOL2 [1] (+6%) although Fe fcc is AFM experimentally and in the databases.

Suiter [96] has computed the total enthalpies at 0 K of 75 pure elements including Fe, Nb and Ni for several phases including bcc\_A2, fcc\_A1, C14, C15 and D8<sub>5</sub>. He listed them in referring to his results for the fcc pure elements. His first-principles calculations use the same method as [93]: the projector augmented wave method (PAW) within the generalized gradient approximation and the Perdew–Wang parameterization GGA-PW91 [94]. That means that he calculated also under the assumption of a possible FM. His results for the enthalpies of formation at 0 K of Fe, Nb and Ni bcc referred to fcc are in good agreement with [93] (−7.7% for Fe, −3.6% for Nb and −4.1% for Ni). We deduced from his results the enthalpies of formation at 0 K of Fe<sub>3</sub> and Nb<sub>3</sub> in C14 and C15 phases referred to FM Fe and NFM Nb bcc\_A2, of Ni<sub>3</sub> C14 and C15 referred to Ni fcc\_A1 and of Nb<sub>13</sub> D8<sub>5</sub> referred to Nb bcc\_A2. They are in good agreement with our AI results.

We did not calculate the AI energy of formation of Fe fcc AFM referred to Fe bcc (FM) and we used, instead, the AI energy of formation of Fe fcc NM referred to Fe bcc (FM). Indeed the AI calculation from Kong and Liu [97] led us to the conclusion that it was not such a bad approximation. Kong and Liu [97] used the Projector Augmented Wave method within the Generalized Gradient Approximation (PAW–GGA). From these authors' AI calculations, we can deduce the energies of formation of Fe fcc AFM state 1 and state 2 referred to Fe fcc NM: −0.1 and +0.1 kJ/mol for respective volumes of 10.283 Å<sup>3</sup> AFM-1, 10.457 Å<sup>3</sup> AFM-2 and 10.245 Å<sup>3</sup> NM – our  $V(\text{Fe fcc NM}) = 10.296 \text{ Å}^3$ . In the case of the energy of formation of Fe fcc FM (high-spin and low-spin) referred to Fe fcc NM, they obtain respectively +1.5 and −0.2 kJ/mol (for respectively  $V = 11.981$  and  $10.390 \text{ Å}^3$ ) while we obtain 0.5 kJ/mol (for  $V = 10.296 \text{ Å}^3$ ). Besides their enthalpy of formation of Fe fcc (high-spin) FM referred to Fe bcc FM is the same as ours: 15.1 kJ/mol.

Table 2 proposes on one hand a comparison between our ab-initio results and the ab-initio results from the literature and on the other hand, a comparison between our ab-initio results after taking into account the purely magnetic enthalpy of Fe and Ni and the optimized or estimated coefficients A selected for the binaries. It appears that, on one hand, our ab-initio calculations and most of the ones from literature are in good agreement except for NiNb<sub>3</sub> L1<sub>2</sub> from Huang et al. [72] and that on the other hand, our ab-initio calculations after the magnetic “correction” and all the optimized A (enthalpy of formation at 0 K) of the CEF compounds are in agreement. That is the case for Ni<sub>3</sub>Nb D0<sub>a</sub>, Fe<sub>2</sub>Nb C14 and FeNi<sub>3</sub> L1<sub>2</sub>. Besides our AI evaluation of the energy of formation of NiNb<sub>3</sub> L1<sub>2</sub> is in good agreement with the optimized value from Du et al. [73]. On the other hand, although our AI value for the energy of formation of NbNi<sub>3</sub> L1<sub>2</sub> is only slightly higher than the energy of formation obtained by [46], it is only two thirds of the one from [72]. Besides it leads to an enthalpy of formation referred to the GHSER about double the value optimized by [73]. Comparing the magnetic moments of the literature and of our AI calculation, rises the problem of the type of magnetism of the C14 Laves (especially of Fe<sub>2</sub>Nb) and of the approximation used in our TDB that the magnetic properties of L1<sub>2</sub> are simply equal to the ones of fcc\_A1. It has also to be noticed that the discrepancies between the AI energies at 0 K and the enthalpic A value for metastable CEF compounds can be very big, even if one knows that at the same time the impact is small on optimization. It has to be pointed out also that NbNi<sub>3</sub> and VNi<sub>3</sub> D0<sub>22</sub> have similar enthalpies of formation, which could be interpreted as a behavior similar enough to Nb and V.

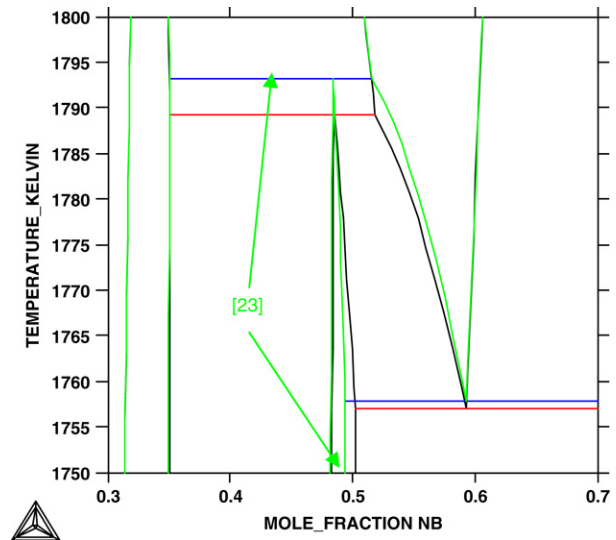


Fig. 6. Zoom of the Fe–Nb phase diagram on the composition domain involving the D8<sub>5</sub> phase. Comparison between the one calculated thanks to our adjusted parameters for D8<sub>5</sub> modelled with a two-sublattice model and the one calculated thanks to the parameters from Toffolon and Servant [23] with a four-sublattice model for D8<sub>5</sub>.

## 4. Calphad-type optimization

### 4.1. The binary Fe–Nb (adjustment)

Starting from the selected optimization from Toffolon and Servant [23], the D8<sub>5</sub> ( $\mu$ ) parameters in the Fe–Nb binary system were simply adjusted with a two-sublattice description, in order to reproduce their phase diagram, which can be seen on Fig. 6. We simply amended the binary interaction parameters <sup>0</sup>L and <sup>1</sup>L for this phase, keeping for the Gibbs energy of formation of the end member Fe<sub>7</sub>Nb<sub>6</sub> the same as optimized by [23] in the case of the four-sublattice model. The new and previous assessments are compared in Fig. 6.

Our calculated invariant reactions (temperature and composition) not including D8<sub>5</sub> are of course the same as [23]. Our calculated invariant reaction, temperature and composition, including D8<sub>5</sub> are about the same as [23]. But our peritectic, D8<sub>5</sub> ⇌ C14 + liquid is slightly lower than [23] (see Table 3).

### 4.2. Our final choices for all the CEF compounds

Table 2 also presents our final choices for the enthalpies at 0 K of all the CEF compounds.

As mentioned above, despite some possible disagreements between the AI starting hypothesis of magnetism and the “real” (experimental or virtual) ones, our AI calculations of enthalpies are in agreement with those (estimated or optimized) from the literature at 0 K. Besides, our AI enthalpies and magnetic moments and the AI ones proposed by other authors have at least the same order of magnitude.

We decided to ignore the discrepancy between AI calculations and our selected values for the unary CEF compounds and for some of the antistructure CEF compounds. For C14, C15, D8<sub>5</sub> and D0<sub>a</sub>, we kept generally the idea that Fe and Ni would behave similarly. We noticed that for C14 the AI enthalpy of Fe<sub>2</sub>Nb and Ni<sub>2</sub>Nb are almost the same. Therefore we choose for the Ni<sub>2</sub>Nb C14 the same value optimized by [23] for Fe<sub>2</sub>Nb C14. For C15, we made the choice to deduce the enthalpy of formation of C15 Fe<sub>2</sub>Nb by using the AI NM calculation from Asano and Ishida [80]. Besides, as our AI

**Table 2**

Enthalpies of formation at 0 K of the end-members of the stable and metastable phases of the Fe–Nb–Ni system; our final choices of enthalpies at 0 K. A of our TDB, (magnetic effect excluded for the pure elements references) for all the CEF compounds; the A deduced from our AI results; the other possible A from the literature; the magnetic moments entered in our TDB; the magnetic moment obtained from our AI calculations; the ones proposed in the literature; our AI energies at 0 K including the magnetic effect of the pure elements references; the ones from the literature. The numbers (n) are for magnetism: (1) = FM (or NFM); (2) = NM; (3) = AFM; (4) = PM.

Name used in the publication for the phase	CEF compounds	Our TDB: Optimized or estimated A J/mol. from literature or from this work	This work: Ab-initio $\Delta H$ J/mol referred to GHSER	Literature Other found A	Our TDB: $\beta$ ( $\mu_B$ )	This work: Ab-initio $\beta$ ( $\mu_B$ )	Literature: Exp. or estim. or Ab-initio $\beta$ ( $\mu_B$ )	This work: Ab-initio $\Delta H$ J/mol referred to elements FM (or NFM)	Literature Ab-initio $\Delta H$ J/mol referred to elements FM (or NFM)
D8 <sub>5</sub>									
Metastable	Nb <sub>13</sub>	65000 [17]	209344 (1)	65000 [15] 234000 (1) [96]	0	0 (1)	-	209344 (1)	234000 (1) [96]
Stable	Nb <sub>6</sub> Fe <sub>7</sub>	-305500 ref. Fe fcc i.e. -315736.80 ref. Fe bcc (T < 1811 K) [23]	-239598 (1)	-305500 ref. Fe fcc i.e. -315736.80 ref. Fe bcc (T < 1811 K) [23] -290033.3 [23] -165463.87 [15] -169771.16 [15]	0	8.62 (1)	20.65 ± 0.35 (3) exp. [24]	-175676 (1)	
Stable	Nb <sub>6</sub> Ni <sub>7</sub>	-312097.5 [17]	-295532 (1)	-	0	0.1 (1)	-	-280241 (1)	-
D0 <sub>16</sub>									
Metastable	Fe <sub>4</sub>	20000	-3967	-	0	0 (1)	-	32560 (1)	
Metastable	Nb <sub>4</sub>	20000 [17]	74948	-	0	0 (1)	-	74948 (1)	
Metastable	Ni <sub>4</sub>	20000 [17]	488	+ 62962.56 [41]	0	2.54 (1)	-	9226 (1)	
Metastable	Fe <sub>1</sub> Nb <sub>3</sub>	48500	-6260 (1)	-	0	0 (1)	-	2871 (1)	
Metastable	Fe <sub>1</sub> Ni <sub>3</sub>	20000	-6291 (2)	-	0	4.6 (1)	-	2841 (2)	
Stable	Nb <sub>1</sub> Ni <sub>3</sub>	-141202.4 [17]	+48975 (2) -127831 (1 and 2)	-17726.2 [41] -140406 (2) deduced from [46]	0	0 (1)	(4) exp. VT [25] (4) exp. at least since 1.5 K [45]	+64660 (2) -121261 (1 and 2)	-133836 (2) [46]
Metastable	Nb <sub>1</sub> Fe <sub>3</sub>	-8500	-8523 (1) 4941 (2)	-	0	2.6 (1)	-	18872 (1) 32336 (2)	
Metastable	Ni <sub>1</sub> Fe <sub>3</sub>	20000	-18890 (1) +136746 (2)	-	0	8.7 (1)	-	10689 (1) 166326 (2)	
Metastable	Ni <sub>1</sub> Nb <sub>3</sub>	181202.3 [17]	5627 (1 and 2)	-	0	0 (1)	-	7811 (1 and 2)	
D0 <sub>22</sub>									
Metastable	Fe <sub>4</sub>	20000	-37360 (1) 147193 (2)	-	0	8.8 (1)	8.8–10.4 (1) estimated from exp. by [48]	-834 (1) 183720 (2)	
Metastable	Nb <sub>4</sub>	20000	279 (1)	+ 88000 [49] V <sub>4</sub> : +32000 [50]	0	0 (1)	-	279 (1)	
Metastable	Ni <sub>4</sub>	20000	27044 (1) 33187 (2)	4363.13 [50] 22137 (2) deduced from [58]	0	2.2 (1)	3.2 (1) exp. layers at 4.5 K [57]	35782 (1) 41925 (2)	30875 (2) (MAEM) [58]
Metastable	Fe <sub>1</sub> Nb <sub>3</sub>	94000	-6396 (1)	-	0	0.2 (1)	-	2736 (1)	
Metastable	Fe <sub>1</sub> Ni <sub>3</sub>	20000	-9296 (1)	-	0	4.6 (1)	-	6389 (1)	
Metastable	Nb <sub>1</sub> Ni <sub>3</sub>	-62000	-62279 (1)	Ni <sub>3</sub> V: -51569.39 [50] -51400.39 [50] -15543.68 [50]	0	0 (1)	Ni <sub>3</sub> V: (4) [100]	-55726 (1)	
Metastable	Nb <sub>1</sub> Fe <sub>3</sub>	-54000	-53845 (1)	-	0	5.1 (1)	-	-26450 (1)	
Metastable	Ni <sub>1</sub> Fe <sub>3</sub>	20000	85433 (1)	-	0	3.0 (1)	-	112828 (1)	
Metastable	Ni <sub>1</sub> Nb <sub>3</sub>	102000	5840 (1)	NiV <sub>3</sub> : +51569.3 [50] +87763 [50]	0	0 (1)	-	8025 (1)	

(continued on next page)



Table 2 (continued)

Name used in the publication for the phase	CEF compounds	Our TDB: Optimized or estimated A J/mol. from literature or from this work	This work: Ab-initio $\Delta H$ J/mol referred to GHSER	Literature Other found A	Our TDB: $\beta$ ( $\mu_B$ )	This work: Ab-initio $\beta$ ( $\mu_B$ ) referred to	Literature: Exp. or estim. or Ab-initio $\beta$ ( $\mu_B$ )	This work: Ab-initio $\Delta H$ J/mol referred to elements FM (or NFM)	Literature Ab-initio $\Delta H$ J/mol referred to elements FM (or NFM)
C14									
Metastable	Fe <sub>3</sub>	15000 [23]	89051 (1)	15000 [15] 65905 (1) deduced from [96]	0	0.01 (1)	–	116446 (1)	93300 (1) [96]
Metastable	Nb <sub>3</sub>	15000 [21]	46808 (1)	15000 [15] 46200 (1) [96]	0	0 (1)	–	46808 (1)	46200 (1) [96]
Metastable	Ni <sub>3</sub>	15000 [85]	56058 (1)	54815 (1) deduced from [96]	0	1.8 (1)	–	58243 (1)	57000 (1) [96]
Metastable	Fe <sub>1</sub> Nb <sub>2</sub>	103200 [23]	–2937 (1)	69356.75 [15]	0	0.001 (1)	–	6195 (1)	–
Metastable	Fe <sub>1</sub> Ni <sub>2</sub>	15000	10556 (1)	–	0	4.1 (1)	–	24057 (1)	–
Metastable	Nb <sub>1</sub> Ni <sub>2</sub>	–73200	–62455 (1)	–73605 [101]	0	0 (1)	–	–58086 (1)	–
Stable	Nb <sub>1</sub> Fe <sub>2</sub>	–73200 [23]	–61795 (1)	–45453.24 [15]	0	0.4 (1)	(3) [29] (3) [31] 0.092 (1) exp. [24] 0 (1) Exp. [26] 0 (1) calc. [27]	–43531 (1)	–
Metastable	Ni <sub>1</sub> Fe <sub>2</sub>	15000	34151 (1)	–	0	4.8 (1)	–	54599 (1)	–
Metastable	Ni <sub>1</sub> Nb <sub>2</sub>	103200	158418 (1)	–	0	0 (1)	–	160603 (1)	–
C15									
Metastable	Fe <sub>3</sub>	15000	76500 (1)	62305 (1) deduced from [96]	0	3.4 (1)	–	103895 (1)	89700 (1) [96]
Metastable	Nb <sub>3</sub>	15000 [21]	47111 (1)	48600 (1) [96]	0	0 (1)	–	79794 (1)	48600 (1) [96]
Metastable	Ni <sub>3</sub>	15000	54131 (1)	52346 (1) deduced from [96]	0	1.7 (1)	–	65685 (1)	63900 (1) [96]
Metastable	Fe <sub>1</sub> Nb <sub>2</sub>	97686.5	216682 (1)	–	0	0 (1)	–	225814 (1)	–
Metastable	Fe <sub>1</sub> Ni <sub>2</sub>	15000	15275 (1)	–	0	4.1 (1)	–	28775 (1)	–
Metastable	Nb <sub>1</sub> Ni <sub>2</sub>	–67686.5	–58788 (1)	–60000 [101]	0	1 (1)	–	–54419 (1)	–
Metastable	Nb <sub>1</sub> Fe <sub>2</sub>	–67686.5	–61255 (1)	–67686.5 deduced from [23] + [80] (2)	0	2.4 (1)	–	–42991 (1) $\Delta H(C15-C14) = 540$ (1)	$\Delta H(C15-C14) = 5513.5$ (2) [80] $\Delta H(C15-C14) = 905$ (1) [80] $\Delta H(C15-C14) = 9053$ (3) [80]
Metastable	Ni <sub>1</sub> Fe <sub>2</sub>	15000	30979 (1)	–	0	4.9 (1)	–	51427 (1)	–
Metastable	Ni <sub>1</sub> Nb <sub>2</sub>	97686.5	145736 (1)	–	0	0 (1)	–	147920 (1)	–
L1 <sub>2</sub>									
Metastable	Fe <sub>0.25</sub> Nb <sub>0.75</sub>	–12141	2968 (1)	–28815 [64]	0.175 (3)	0 (1)	–	30235 (1)	–
Stable	Fe <sub>0.25</sub> Ni <sub>0.75</sub>	–14400 [63,62]	–12700 (1)	–10895.7 (1) [71] –11699 (1) [69] –12485.4 (1) [70] 17666.7 (2) [70]	1.11 (1)	1.2 (1)	1.20 (1) [69] $\Delta(\beta L12-fcc) = 0.115$ (1) [38] 1.228 (1) [70]	–8802 (1)	–7613.83 (1) [71] –8587.06 (1) [69] –9455.7 (1) [70] 20696.4 (2) [70]

Table 2 (continued)

Name used in the publication for the phase	CEF compounds	Our TDB: Optimized or estimated A J/mol. from literature or from this work	This work: Ab-initio $\Delta H$ J/mol referred to GHSER	Literature Other found A	Our TDB: $\beta$ ( $\mu_B$ )	This work: Ab-initio $\beta$ ( $\mu_B$ )	Literature: Exp. or estim. or Ab-initio $\beta$ ( $\mu_B$ )	This work: Ab-initio $\Delta H$ J/mol referred to elements FM (or NFM)	Literature Ab-initio $\Delta H$ J/mol referred to elements FM (or NFM)
Metastable	Nb <sub>0.25</sub> Ni <sub>0.75</sub>	–12 141 [73]	–22613 (1)	–31432 (1) deduced from [72] –25009.2 (2) deduced from [46]	0.39 (1)	0.2 (1)	Ni <sub>3</sub> V: 0.33 (1) [100]	–14820 (1)	–23639 (1) [72] –17216.2 (2) [46]
Metastable	Nb <sub>0.25</sub> Fe <sub>0.75</sub>	–12 141	–17854 (1)	–	0.525 (1)	0.9 (1)	–	1629 (1)	–
Metastable	Ni <sub>0.25</sub> Fe <sub>0.75</sub>	9171 [63,62]	–7808 (1)	–16500 [64] –3281.8 (1) [71] –4703.7 (1) [69] –6213.7 (1) [70] 20860.4 (2) [70] –25300 deduced from [72]	1.45 (1)	2.1 (1)	2.07 (1) [69] 2.14 (1) [70]	3884 (1)	6563.65 (1) [71] 4631.22 (1) [69] 2875.3 (1) [70] 29949.4 (2) [70]
Metastable	Ni <sub>0.25</sub> Nb <sub>0.75</sub>	–12 141 [73]	–14378 (1)	–	0.13 (1)	0 (1)	–	8992 (1)	–1930 (1) [72]

\* MAEM is not exactly an ab-initio method but this result is anyway presented here for convenience.

**Table 3**

Invariant reaction temperatures (K): comparison between the calculated invariant temperatures from the present work, Toffolon and Servant [23], Coelho et al. [15] and the experimental data from Zelaya et al. [19].

Invariant equilibrium	Present work	(Four-sublattices) [23]	(Two-sublattice) [15]	Experimental [19]
Peritectoid: bcc#1 $\leftrightarrow$ fcc + C14	1215	1215	1232	1233
Eutectoid: fcc + C14 $\leftrightarrow$ bcc#1	1472	1472	1463	1463
Eutectic: bcc#1 + C14 $\leftrightarrow$ Liq.	1667	1667	1646	1643
CongruentMelting: C14 $\leftrightarrow$ Liq.	1904	1904	1920	1903
Peritectic: D8 <sub>5</sub> $\leftrightarrow$ C14 + Liq.	1789	1793	1795	1793
Eutectic: D8 <sub>5</sub> + bcc#2 $\leftrightarrow$ Liq.	1757	1758	1771	1773

enthalpies for C15 Ni<sub>2</sub>Nb and Fe<sub>2</sub>Nb have almost the same value, we introduce the same value for both compounds in the TDB. In the case of D0<sub>22</sub>, in order to be consistent with the modelling of D0<sub>a</sub>, and as we could not adjust any experimental data, we introduced arbitrarily, for the pure elements, Gibbs energies independent of the temperature with a value of 5000 kJ/mol per atom. We also chose to keep a reciprocal model based on our AI calculation for Fe<sub>3</sub>Nb and Ni<sub>3</sub>Nb. For Fe<sub>3</sub>Nb L1<sub>2</sub>, we noticed that its AI enthalpy of formation at 0 K was more or less of the same order of magnitude as the one we obtained for Ni<sub>3</sub>Nb L1<sub>2</sub>. Therefore, we introduce for Fe–Nb L1<sub>2</sub>, the parameters proposed by Du et al. [73] for Ni–Nb L1<sub>2</sub>.

#### 4.3. Calphad-type optimization of the ternary Fe–Nb–Ni system excluding L1<sub>2</sub>

As we mentioned above, the general idea of our study was on one hand to try to use ab-initio data for optimization work, in particular because we have to cope with metastable phases. On the other hand our aim was to represent reasonably well the different experimental data at different temperatures with a minimum number of parameters to be optimized, in order to build a quaternary database Cr–Fe–Nb–Ni as simply as possible

Anyway many parameters (like the interaction parameters of two elements on each sublattice) other than the enthalpies of formation at 0 K had to be estimated. We assumed most of the time that Fe and Ni behaved similarly and in the case of C15, even similarly as Cr in Cr–Nb C15 from Costa et al. [21]. We set the entropy of formation of Fe<sub>3</sub>Nb D0<sub>22</sub> and D0<sub>a</sub> equal which made, at 1500 K, the Gibbs energy of formation of Fe<sub>3</sub>Nb D0<sub>a</sub> of the same order of magnitude as for Cr<sub>3</sub>Nb D0<sub>a</sub> [22] and destabilised Fe<sub>3</sub>Nb D0<sub>22</sub> on the binary. It should be noted that the Gibbs energies of formation we chose for Ni<sub>2</sub>Nb C14 and C15 are equal respectively to the one of Fe<sub>2</sub>Nb C14 [23] and of the one we deduced for Fe<sub>2</sub>Nb C15 from [80] combined at [23]. Besides, the entropy of formation of Fe<sub>2</sub>Nb C15 (and so of Ni<sub>2</sub>Nb C15) we introduced is the one we “optimized” for Fe<sub>2</sub>Nb C15 in Cr–Fe–Nb [22].

These assumptions correspond respectively to:

- \* for a phase  $\phi$  = C14 (or C15):  $\Delta G^{\text{form.}}(\phi, \text{Fe:Ni}) = \Delta G^{\text{form.}}(\phi, \text{Fe:Fe}) = \Delta G^{\text{form.}}(\phi, \text{Ni:Ni}) = \Delta G^{\text{form.}}(\phi, \text{Ni:Fe}) = 15000$ ,
- \* for a phase  $\phi$  = C14, D0<sub>a</sub>, D8<sub>5</sub> (or C15), and A = Fe, Nb or Ni:  $L(\phi, \text{A:Fe, Ni}) = 0 = L(\phi, \text{Fe, Ni:A})$  except  $L(\text{C14, Fe, Ni:Nb})$  that has been optimized,
- \* for a phase  $\phi$  = C14, C15 or D0<sub>a</sub>:  $L(\phi, *: \text{Fe, Nb}) = L(\phi, *: \text{Nb, Ni})$  and  $L(\phi, \text{Fe, Nb:}*) = L(\phi, \text{Nb, Ni:}*)$  except  $L(\text{D0}_a, \text{Fe, Nb:Ni})$  that has been optimized,
- \*  $\Delta S^{\text{form.}}(\text{D0}_{22}, \text{Nb:Fe}) = \Delta S^{\text{form.}}(\text{D0}_a, \text{Nb:Fe})$  so that  $\Delta G^{\text{form.}}(\text{D0}_a, \text{Nb:Fe}) \approx \Delta G^{\text{form.}}(\text{D0}_a, \text{Nb:Cr})$  at 1500 K [22],
- \*  $\Delta G^{\text{form.}}(\text{C14, Ni:Nb}) = \Delta G^{\text{form.}}(\text{C14, Fe:Nb})$  from [23] and  $\Delta G^{\text{form.}}(\text{C15, Ni:Nb}) = \Delta G^{\text{form.}}(\text{C15, Fe:Nb})$  deduced from [23, 80],
- \*  $\Delta S^{\text{form.}}(\text{C15, Ni:Nb}) = \Delta S^{\text{form.}}(\text{C15, Fe:Nb})$  from [22].

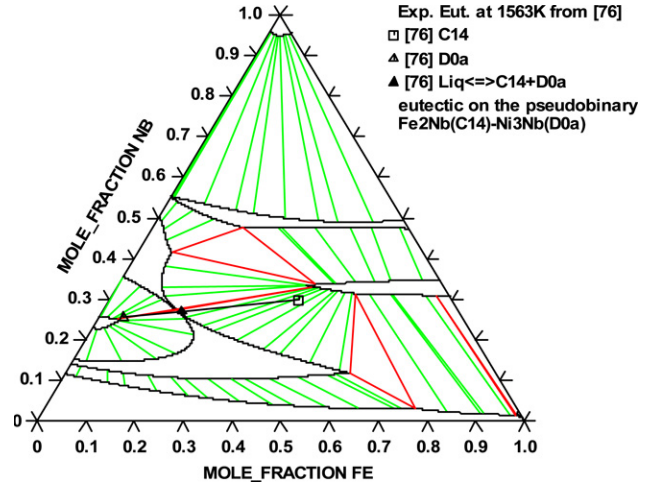


Fig. 7. Isothermal section at 1564.05 K of the Fe–Nb–Ni ternary phase diagram. Comparison with the pseudobinary eutectic from Panteleimonov and Aleshina [76] at 1563 K.

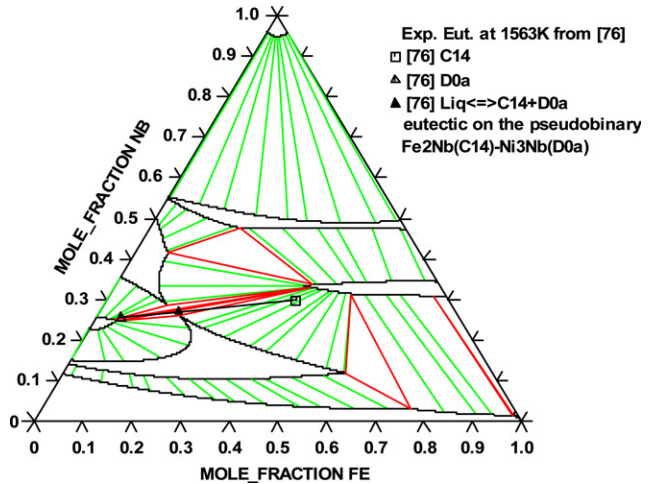


Fig. 8. Isothermal section at 1563 K of the Fe–Nb–Ni ternary phase diagram.

All the available phase diagram data have been taken into account in the optimization with various weights. Solubility limits from tie-lines have not been always entered together as some tie-lines could be contradictory while the solubility limits could still be inside the uncertainties used in the optimization.

We did not try to fit absolutely the data from [8] for the ternary C14 at 1473 K as we could not re-assess the binary Fe–Nb.

We performed our optimization without any ternary mixing parameters for the liquid and without taking into account the pseudo-binary eutectic found at 1563 K by [76] (16.2% Fe–27% Nb–56.8% Ni Liq.  $\leftrightarrow$  38.8% Fe–29.8% Nb–31.4% Ni C14 + 5.1% Fe–25.6% Nb–69.3% Ni D0<sub>a</sub>) nor the presence of liquid

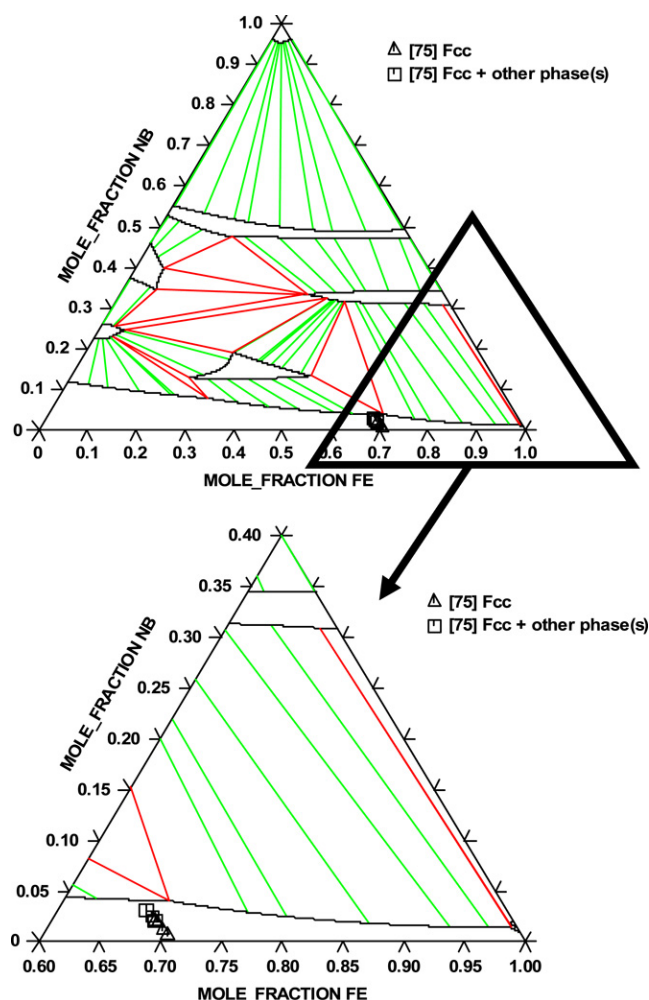


Fig. 9. Isothermal section at 1523 K of the Fe–Nb–Ni ternary phase diagram.

from [7] at 1473 K (25% Fe–20% Nb–55% Ni liquid). Therefore we obtained:

- an eutectic at 1477.07 K: 39.9% Fe–15.1% Nb–45% Ni Liq.  $\leftrightarrow$  45% Fe–31.8% Nb–23.2% Ni C14 + 6.2% Fe–24.4% Nb–69.4% Ni D0<sub>a</sub> + 58.2% Fe–5.9% Nb–35.9% Ni fcc\_A1, but for a liquid composition too rich in Fe and not enough in Nb or Ni compared to the liquid composition of [7],
- and a pseudobinary invariant at 1564.05 K: 14.9% Fe–27.4% Nb–57.7% Ni Liq.  $\leftrightarrow$  39.8% Fe–33.1% Nb–27.1% Ni C14 + 4.2% Fe–25.1% Nb–70.7% Ni D0<sub>a</sub>.

Figs. 7–13 show several isothermal sections between 1564.05 and 1073 K. Comparisons with the experimental data at 1564.05, 1563, 1523, 1473, 1273, 1223 and 1073 K show that most of the different equilibrium fields are respected despite the experimental uncertainties and disagreements. It has to be noticed that despite the ambiguity of the data from [6], we took into account in our calculation some of them: the ones not presenting any disagreement with a first optimization performed without them.

The corresponding TDB is listed in Appendix B.

#### 4.4. The L<sub>12</sub> and D0<sub>22</sub> phases

Some of the L<sub>12</sub> CEF end members have been found to be magnetic. But as already mentioned, the magnetic properties of L<sub>12</sub> have been treated as those of fcc\_A1.

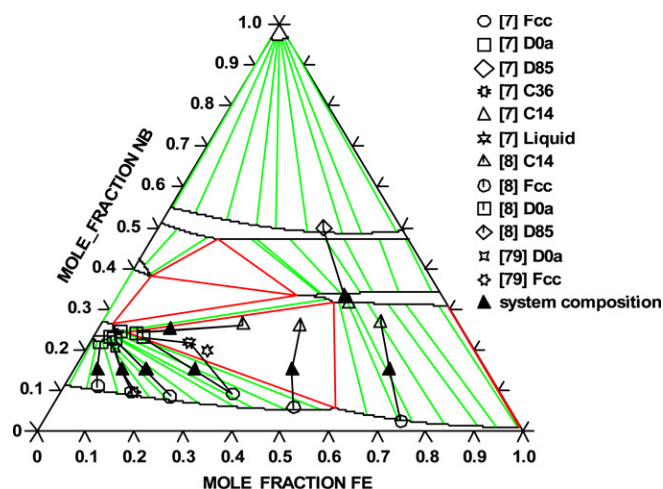


Fig. 10. Isothermal section at 1473 K of the Fe–Nb–Ni ternary phase diagram.

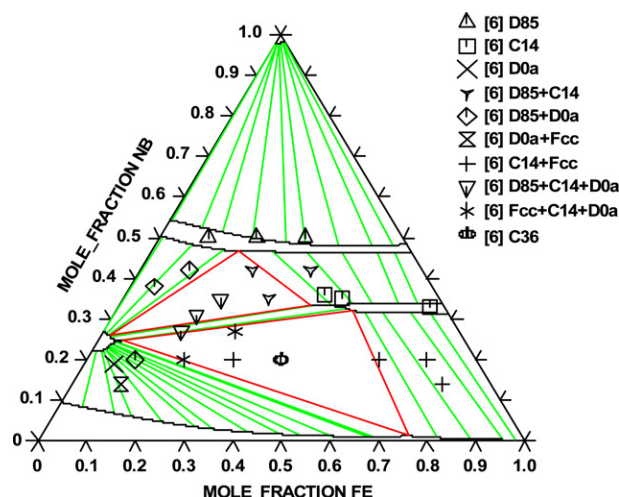


Fig. 11. Isothermal section at 1273 K of the Fe–Nb–Ni ternary phase diagram.

Our L<sub>12</sub> phase description is based on the Fe–Ni L<sub>12</sub> optimization from Ansara [63] published by Servant et al. [62], on the Nb–Ni L<sub>12</sub> optimization from Du et al. [73] and on our evaluations of metastable end members for Fe–Nb L<sub>12</sub>. The ternary corrective terms [86,59] necessary to obtain a correctly disordered state have been entered. Besides two supplementary modifications had to be done due to the asymmetry of the modelization of L<sub>12</sub> on the Fe–Ni binary compared to the Fe–Nb and Ni–Nb ones. The ternary parameter  $L(L_{12}, \text{Nb} : \text{Fe}, \text{Ni})$  was set equal to  $L(L_{12}, \text{Fe} : \text{Fe}, \text{Ni})$  and the ternary  $L(L_{12}, \text{Fe}, \text{Ni} : \text{Nb})$  includes additively 3 times the binary interaction  $L(L_{12}, \text{Fe} : \text{Fe}, \text{Ni})$  (see Appendix B). These relations can be derived from the requirement that the disordered state should be stable at high temperature. Fig. 14 presents an isothermal section of the Fe–Nb–Ni phase diagram at 723 K.

Although some of the CEF compounds have been found magnetic by ab-initio calculation, due to the lack of data, in particular on the magnetic transformation temperatures, we did not introduce in the TDB any magnetism for the D0<sub>22</sub> phase. In fact, at this step, nothing more than a first estimation of the Gibbs energies of the CEF compounds has been done for D0<sub>22</sub>, due to the lack of useful data in this ternary. Useful experimental results for optimizations including D0<sub>22</sub> include also an L<sub>12</sub> based on Ni<sub>3</sub>(Al, Nb, Ti) largely richer in Al (or Ti) than in Nb. The introduction of Al as fifth element in the TDB is then necessary.



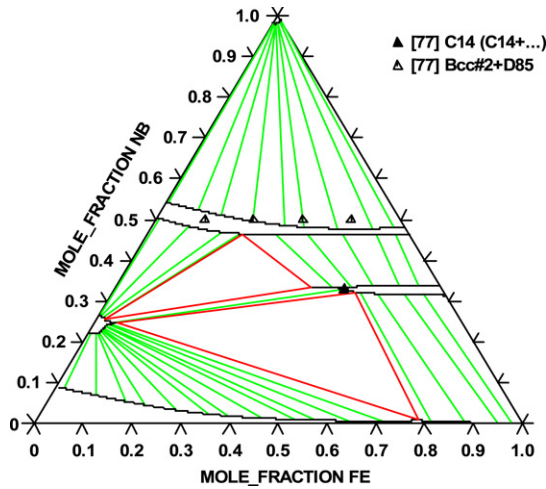


Fig. 12. Isothermal section at 1223 K of the Fe-Nb-Ni ternary phase diagram.

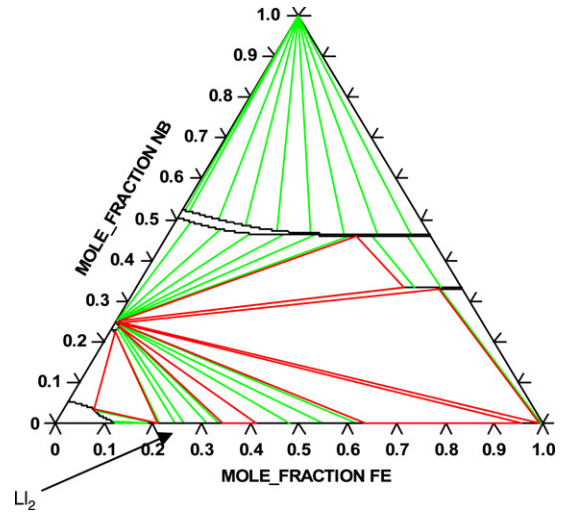


Fig. 14. Isothermal section at 723 K of the ternary Fe-Nb-Ni phase diagram.

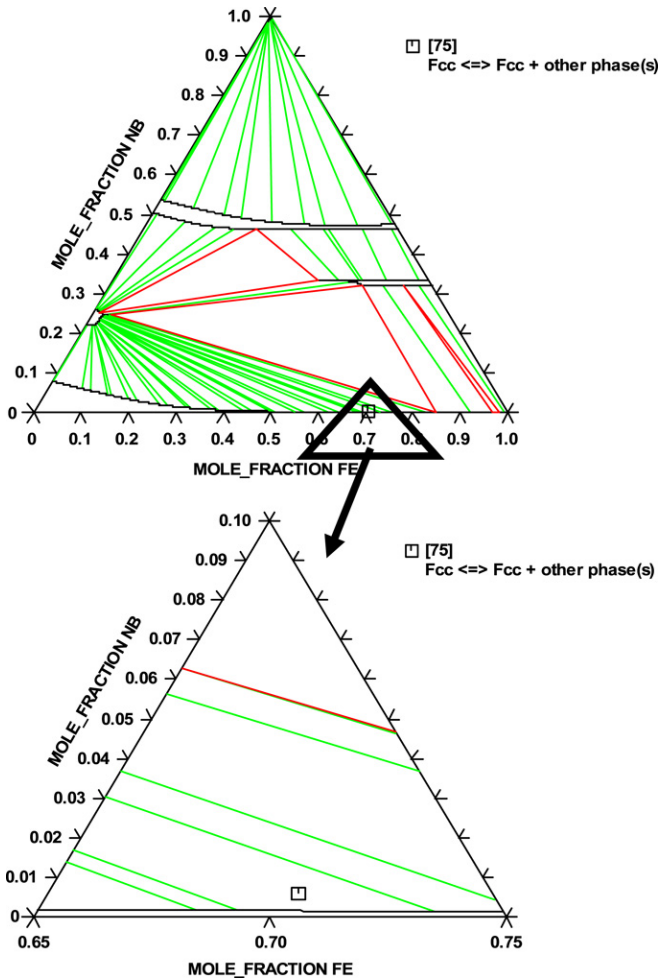


Fig. 13. Isothermal section at 1073 K of the Fe-Nb-Ni ternary phase diagram.

## 5. Conclusion

The systematic ab-initio simulations, performed in our study, for all the CEF compounds encountered in the Fe-Nb-Ni ternary, provided food for thought on the possibilities of using them for a Calphad-type optimization. This is the case, in particular,

because it pointed out, on one hand, good agreement with the optimized enthalpies at 0 K for all the stable CEF compounds but, on the other hand, for most of the antistructures and metastable element structures, big discrepancies with the estimated or optimized enthalpies at 0 K. It also emphasized the importance of assumptions on magnetism.

Besides, in the perspective of building a quaternary database Cr-Fe-Nb-Ni as simple as possible, the Gibbs energies of the stable or metastable phases, liquid, bcc\_A2, fcc\_A1, D0<sub>a</sub>, D8<sub>5</sub>, C14, C15 of the ternary Fe-Nb-Ni system have been determined with a minimum of optimized parameters. In the case of L1<sub>2</sub>-fcc and D0<sub>22</sub>, no adjustment could be made due to an absence of useful experimental data.

## Acknowledgments

The authors would like to acknowledge the Midi-Pyrénées region for its financial support, the Calmip CICT Toulouse supercomputer facilities and Dr. Helena Federova for her translation of the Russian and Ukrainian publications.

## Appendix A. Formula of the Gibbs energy, versus temperature and composition, and magnetism model

*Substitutional model for disordered solid solutions (liquid, fcc\_A1, bcc\_A2):*

$$\Delta G_m^\varphi(x_i^\varphi, T) = \sum_i x_i^\varphi \Delta G_i^\varphi(T) + RT \sum_i x_i^\varphi \ln(x_i^\varphi) + \sum_i \sum_{j \neq i} x_i^\varphi x_j^\varphi L_{i,j}^\varphi + x_i^\varphi x_j^\varphi x_k^\varphi L_{i,j,k}^\varphi$$

$$\text{with } L_{i,j}^\varphi = \sum_n {}^n L_{i,j}^\varphi(T) (x_i^\varphi - x_j^\varphi)^n \quad \text{and} \quad L_{i,j,k}^\varphi = \sum_{l=i,j,k} {}^l L_{i,j,k}^\varphi(T) x_l^\varphi$$

$$\text{with } {}^n L^\varphi(T) = A + BT + \dots$$

*Compound Energy Formalism for a two-sublattice model (i, j, k)<sub>a</sub>(i, j, k)<sub>b</sub>: (phases C14, C15, D0<sub>a</sub>, D0<sub>22</sub>), for y<sub>i</sub><sup>s,φ</sup> the site fraction of the sublattice s (s = 1 or 2):*

$$\Delta G_m^\varphi(y_i^{s,L12}, T) = \sum_i \sum_j y_i^{1,\varphi} y_j^{2,\varphi} \Delta G_{ij}^\varphi(T) + RT \left[ a \sum_i y_i^{1,\varphi} \ln(y_i^{1,\varphi}) + b \sum_i y_i^{2,\varphi} \ln(y_i^{2,\varphi}) \right]$$

$$+ \sum_i \sum_{j \neq i} \sum_k y_i^{1,\varphi} y_j^{1,\varphi} y_k^{2,\varphi} L_{i,j,k}^\varphi + \sum_i \sum_{j \neq i} \sum_k y_k^{1,\varphi} y_i^{2,\varphi} y_j^{2,\varphi} L_{k,i,j}^{L12} \\ + \sum_i y_i^{1,\varphi} y_j^{1,\varphi} y_k^{1,\varphi} y_l^{2,\varphi} L_{i,j,k,l}^\varphi + \sum_i y_l^{1,\varphi} y_i^{2,\varphi} y_j^{2,\varphi} y_k^{2,\varphi} L_{l,i,j,k}^\varphi + \dots$$

$$\text{with } L_{i,j,k}^\varphi = \sum_n^n L_{i,j,k}^\varphi(T) (y_i^{1,\varphi} - y_j^{1,\varphi})^n$$

$$\text{and } L_{k,i,j}^\varphi = \sum_n^n L_{k,i,j}^\varphi(T) (y_i^{2,\varphi} - y_j^{2,\varphi})^n.$$

The case of the order phase L1<sub>2</sub>:

$$\Delta G_m^{L12}(y_i^{s,L12}, T) = \sum_i \sum_j y_i^{1,L12} y_j^{2,L12} \Delta G_{i,j}^{L12}(T) \\ + RT \left[ 0.75 \sum_i y_i^{1,L12} \ln(y_i^{1,L12}) + 0.25 \sum_i y_i^{2,L12} \ln(y_i^{2,L12}) \right] \\ + \sum_i \sum_{j \neq i} \sum_k y_i^{1,L12} y_j^{1,L12} y_k^{2,L12} L_{i,j,k}^{L12} \\ + \sum_i \sum_{j \neq i} \sum_k y_k^{1,L12} y_i^{2,L12} y_j^{2,L12} L_{k,i,j}^{L12} \\ + \sum_i y_i^{1,L12} y_j^{1,L12} y_k^{1,L12} y_l^{2,L12} L_{i,j,k,l}^{L12} \\ + \sum_i y_l^{1,L12} y_i^{2,L12} y_j^{2,L12} y_k^{2,L12} L_{l,i,j,k}^{L12} + \dots$$

with

$$\Delta G_m^{\text{Fcc or } L12} = \Delta G_m^{\text{Fcc}}(x_i^{\text{Fcc or } L12}, T) + \Delta G_m^{\text{only ord., } L12}(y_i^{s,L12}, T) \\ = \Delta G_m^{\text{Fcc}}(x_i^{\text{Fcc or } L12}, T) + \Delta G_m^{L12}(y_i^{s,L12}, T) \\ - \Delta G_m^{L12}(y_i^{s,L12} = x_i^{\text{Fcc or } L12}, T)$$

$$\text{with } L_{i,j,k}^{L12} = \sum_n^n L_{i,j,k}^{L12}(T) (y_i^{1,L12} - y_j^{1,L12})^n$$

$$\text{and } L_{k,i,j}^{L12} = \sum_n^n L_{k,i,j}^{L12}(T) (y_i^{2,L12} - y_j^{2,L12})^n.$$

### Magnetism

The magnetic contribution to the Gibbs energy was first proposed by Inden [98] and modified later on by Hillert and Jarl [99].

The  $T_C^{\text{TDB or calc.}}$  and  $\beta^{\text{TDB or calc.}}$  calculated from the parameters in the TDB mean respectively the Curie temperature and the magnetic moment, only in the case of positive values. If the  $T_C^{\text{TDB or calc.}}$  and the  $\beta^{\text{TDB or calc.}}$  are negative, they are proportional respectively to the Néel temperature and the corresponding magnetic moment.

In the case of ferromagnetism, the second-order transition temperature and the magnetic moment, plotted (plot.) or introduced (intro.) in the Gibbs energy formula, are directly calculated from the values in the TDB. In the case of antiferromagnetism, the second-order transition temperature and the magnetic moment, plotted (plot.) or introduced (intro.) in the Gibbs energy formula, are then of course the deduced Néel Temperature and corresponding magnetic moment.

Case of  $\phi$  ferromagnetic (for  $T \leq T_C^{\text{exp}}$ ) at least on a certain composition field:

$$T_C^{\text{TDB or calc. or plot. or intro.}}(\text{phase } \phi \neq \text{bcc or } = \text{bcc}) \\ = T_C^{\text{exp}}(\text{phase } \phi \neq \text{bcc or } = \text{bcc}) \\ \beta^{\text{TDB or calc. or plot. or intro.}}(\text{phase } \phi \neq \text{bcc or } = \text{bcc}) \\ = \beta^{\text{exp}}(\text{phase } \phi \neq \text{bcc or } = \text{bcc}).$$

Case of  $\phi$  antiferromagnetic (for  $T \leq T_{\text{Néel}}^{\text{exp}}$ ) at least on a certain composition field:

$$T_C^{\text{TDB or calc.}}(\text{phase } \phi \neq \text{bcc}) = -3 * T_{\text{Néel}}^{\text{exp}}(\text{phase } \phi \neq \text{bcc}) \\ \beta^{\text{TDB or calc.}}(\text{phase } \phi \neq \text{bcc}) = -3 * \beta^{\text{exp}}(\text{phase } \phi \neq \text{bcc}) \\ \text{But } T_C^{\text{plot. or intro.}}(\text{phase } \phi \neq \text{bcc}) = T_{\text{Néel}}^{\text{exp}}(\text{phase } \phi \neq \text{bcc}) \\ \beta^{\text{plot. or intro.}}(\text{phase } \phi \neq \text{bcc}) = \beta^{\text{exp}}(\text{phase } \phi \neq \text{bcc}) \\ T_C^{\text{TDB or calc.}}(\text{phase bcc}) = -T_{\text{Néel}}^{\text{exp}}(\text{phase bcc}) \\ \beta^{\text{TDB or calc.}}(\text{phase bcc}) = -\beta^{\text{exp}}(\text{phase bcc}) \\ \text{But } T_C^{\text{plot. or intro.}}(\text{phase bcc}) = T_{\text{Néel}}^{\text{exp}}(\text{phase bcc}) \\ \beta^{\text{plot. or intro.}}(\text{phase bcc}) = \beta^{\text{exp}}(\text{phase bcc})$$

with for a binary

$$A-B : T_C^{\text{TDB calc.}} = x_A T_{C,A}^{\text{TDB}} + x_B T_{C,B}^{\text{TDB}} + \sum x_A x_B^n T_C^{\text{TDB}} (x_A - x_B)^n$$

and

$$\beta^{\text{TDB calc.}} = x_A \beta_A^{\text{TDB}} + x_B \beta_B^{\text{TDB}} + \sum x_A x_B^n \beta^{\text{TDB}} (x_A - x_B)^n.$$

Therefore in a classical TDB:

$$\Delta G^{\text{TDB form. tot.}} = \Delta G^{\text{TDB form. non magn}}(T) + \Delta G^{\text{TDB form. only magn.}}(T)$$

with:

$$\Delta G^{\text{TDB form non magn.}}(\phi, A_x B_y, T) = A + BT + CT \ln(T) + \dots \\ + x \Delta G^{\text{TDB form non magn.}}(\alpha, A, T) + y \Delta G^{\text{TDB form non magn.}}(\gamma, B, T) \\ = \Delta H^{\text{TDB non magn.}}(\phi, A_x B_y, T) - T \Delta S^{\text{TDB non magn.}}(\phi, A_x B_y, T)$$

and

$$\Delta G^{\text{TDB only magn.}}(\phi, A_x B_y, T) = RT \ln(\beta^{\text{plot. or intro.}} + 1) f(\tau) \\ = \Delta H^{\text{TDB only magn.}}(\phi, A_x B_y, T) - T \Delta S^{\text{TDB only magn.}}(\phi, A_x B_y, T)$$

with  $\tau = T/T_{\text{C or N}}^{\text{plot. or intro.}}$  and

$$f(\tau) = 1 - \frac{1}{Z} \left\{ \frac{79 \cdot \tau^{-1}}{140 \cdot p} + \frac{474}{497} \left( \frac{1}{p} - 1 \right) \left( \frac{\tau^3}{6} + \frac{\tau^9}{135} + \frac{\tau^{15}}{600} \right) \right\} \\ \text{for } \tau = T/T_{\text{C or N}}^{\text{plot. or intro.}} \leq 1$$

or

$$f(\tau) = -\frac{1}{Z} \left\{ \frac{\tau^{-5}}{10} + \frac{\tau^{-15}}{315} + \frac{\tau^{-25}}{1500} \right\} \text{ for } \tau = T/T_{\text{C or N}}^{\text{plot. or intro.}} \geq 1$$

with

$$Z = \left\{ \frac{518}{1125} + \frac{11692}{15975} \left( \frac{1}{p} - 1 \right) \right\}$$

where  $p$  is the ratio of the magnetic enthalpy due to short range ordering to the total amount of magnetic contribution with  $p = 0.4$  for bcc and 0.28 for fcc, Hcp and all others solid solutions.

**Appendix B. The TDB determined in this work**

\$ Database file written 2008- 4-23

\$ From database: USER

ELEMENT /-	ELECTRON_GAS	0.0000E+00	0.0000E+00	0.0000E+00!
ELEMENT VA	VACUUM	0.0000E+00	0.0000E+00	0.0000E+00!
ELEMENT FE	BCC_A2	5.5847E+01	4.4890E+03	2.7280E+01!
ELEMENT NB	BCC_A2	9.2906E+01	5.2200E+03	3.6270E+01!
ELEMENT NI	FCC_A1	5.8690E+01	4.7870E+03	2.9796E+01!

FUNCTION ZEROMU 2.98150E+02 0.0 ; 3.00000E+03 N !

FUNCTION GHSEFE 2.98140E+02 +1225.7+124.134\*T-23.5143\*T\*LN(T)  
 -.00439752\*T\*\*2-5.8927E-08\*T\*\*3+77359\*T\*\*(-1); 1.81100E+03 Y  
 -25383.581+299.31255\*T-46\*T\*LN(T)+2.29603E+31\*T\*\*(-9); 6.00000E+03 N !

FUNCTION GFELIQ 2.98140E+02 +12040.17-6.55843\*T-3.6751551E-21\*T\*\*7  
 +GHSEFE#; 1.81100E+03 Y  
 -10839.7+291.302\*T-46\*T\*LN(T); 6.00000E+03 N !

FUNCTION GHSENB 2.98140E+02 -8519.353+142.045475\*T-26.4711\*T\*LN(T)  
 +2.03475E-04\*T\*\*2-3.5012E-07\*T\*\*3+93399\*T\*\*(-1); 2.75000E+03 Y  
 -37669.3+271.720843\*T-41.77\*T\*LN(T)+1.528238E+32\*T\*\*(-9); 6.00000E+03 N !

FUNCTION GHSENI 2.98140E+02 -5179.159+117.854\*T-22.096\*T\*LN(T)  
 -.0048407\*T\*\*2; 1.72800E+03 Y  
 -27840.655+279.135\*T-43.1\*T\*LN(T)+1.12754E+31\*T\*\*(-9); 3.00000E+03 N !

FUNCTION GNIBCC 2.98150E+02 +8715.084-3.556\*T+GHSENI#; 6.00000E+03 N !

FUNCTION GFEECC 2.98140E+02 -1462.4+8.282\*T-1.15\*T\*LN(T)+6.4E-04\*T\*\*2  
 +GHSEFE#; 1.81100E+03 Y  
 -27098.266+300.25256\*T-46\*T\*LN(T)+2.78854E+31\*T\*\*(-9); 6.00000E+03 N !

FUNCTION GHEXTNB 2.98150E+02 -8519.35+142.048\*T-26.4711\*T\*LN(T)  
 +2.03475E-04\*T\*\*2-3.50119E-07\*T\*\*3+93398.8\*T\*\*(-1); 6.00000E+03 N !

FUNCTION FENBMEMO 2.98150E+02 -4047; 6.00000E+03 N !

FUNCTION ANUFENI 2.98150E+02 345.08; 6.00000E+03 N !

FUNCTION ANGFE3NI 2.98150E+02 9171; 6.00000E+03 N !

FUNCTION ANGFEI3 2.98150E+02 -14400+12.55471\*T; 6.00000E+03 N !

FUNCTION AGFE2NI2 2.98150E+02 +ZEROMU#; 6.00000E+03 N !

FUNCTION U1NBNIDU 2.98150E+02 -4047; 6.00000E+03 N !

FUNCTION FENBM 2.98150E+02 +FENBMEMO#; 6.00000E+03 N !

FUNCTION FENIM 2.98150E+02 +ZEROMU#; 6.00000E+03 N !

FUNCTION NBNIM 2.98150E+02 +U1NBNIDU#; 6.00000E+03 N !

FUNCTION FE3NBM 2.98150E+02 +3\*FENBM#; 6.00000E+03 N !

FUNCTION FENB3M 2.98150E+02 +3\*FENBM#; 6.00000E+03 N !

FUNCTION FE2NB2M 2.98150E+02 +4\*FENBM#; 6.00000E+03 N !

FUNCTION FE3NIM 2.98150E+02 +ANGFE3NI#; 6.00000E+03 N !

FUNCTION FENI3M 2.98150E+02 +ANGFEI3#; 6.00000E+03 N !

FUNCTION FE2NI2M 2.98150E+02 +AGFE2NI2#; 6.00000E+03 N !

FUNCTION NB3NIM 2.98150E+02 +3\*NBNIM#; 6.00000E+03 N !

FUNCTION NBNI3M 2.98150E+02 +3\*NBNIM#; 6.00000E+03 N !

FUNCTION NB2NI2M 2.98150E+02 +4\*NBNIM#; 6.00000E+03 N !

FUNCTION FENBNI2 2.98150E+02 +FENBM#+2\*FENIM#+2\*NBNIM#; 6.00000E+03 N !

FUNCTION FENB2NI 2.98150E+02 +2\*FENBM#+FENIM#+2\*NBNIM#; 6.00000E+03 N !

FUNCTION FE2NBNI 2.98150E+02 +2\*FENBM#+2\*FENIM#+NBNIM#; 6.00000E+03 N !

FUNCTION FENBNI2M 2.98150E+02 +ZEROMU#; 6.00000E+03 N !

FUNCTION FENB2NIM 2.98150E+02 +ZEROMU#; 6.00000E+03 N !

FUNCTION FE2NBNIM 2.98150E+02 +ZEROMU#; 6.00000E+03 N !

TYPE\_DEFINITION % SEQ \*!

DEFINE\_SYSTEM\_DEFAULT ELEMENT 2 !

DEFAULT\_COMMAND DEF\_SYS\_ELEMENT VA /- !

PHASE LIQUID:L % 1 1.0 !

CONSTITUENT LIQUID:L :FE,NB,NI : !



```

PARAMETER G(LIQUID,FE;0) 2.98150E+02 +GFELIQ#; 6.00000E+03 N 1991DINSDA !
PARAMETER G(LIQUID,NB;0) 2.98140E+02 +29781.555-10.816418*T
-3.06098E-23*T**7+GHSERNB#; 2.75000E+03 Y
+30169.902-10.964695*T-1.528238E+32*T**(-9)+GHSERNB#; 6.00000E+03 N
1991DINSDA !
PARAMETER G(LIQUID,NI;0) 2.98140E+02 +11235.527+108.457*T-22.096*T*LN(T) -
.0048407*T**2-3.82318E-21*T**7; 1.72800E+03 Y
-9549.775+268.598*T-43.1*T*LN(T); 3.00000E+03 N 1991DINSDA !
PARAMETER G(LIQUID,FE,NB;0) 2.98150E+02 -48231.518+11.2225*T; 6.00000E+03
N 2000TOFFOL !
PARAMETER G(LIQUID,FE,NB;1) 2.98150E+02 -9786.6216+5.1445*T; 6.00000E+03
N 2000TOFFOL !
PARAMETER G(LIQUID,FE,NB;2) 2.98150E+02 +29181.806-14.6036*T; 6.00000E+03
N 2000TOFFOL !
PARAMETER G(LIQUID,FE,NI;0) 2.98150E+02 -16911+5.1622*T; 6.00000E+03
N 1993LEE !
PARAMETER G(LIQUID,FE,NI;1) 2.98150E+02 +10180-4.146656*T; 6.00000E+03
N 1993LEE !
PARAMETER G(LIQUID,NB,NI;0) 2.98150E+02 -80037.3-6.31498*T; 6.00000E+03
N 1996BOLCAV !
PARAMETER G(LIQUID,NB,NI;1) 2.98150E+02 +97884.9-19.01069*T; 6.00000E+03
N 1996BOLCAV !
PARAMETER G(LIQUID,NB,NI;2) 2.98150E+02 10000; 6.00000E+03 N
1996BOLCAV !
PARAMETER G(LIQUID,FE,NB,NI;0) 2.98150E+02 +ZEROMU#; 6.00000E+03 N
2008MEMO !

```

```

TYPE_DEFINITION & GES A_P_D BCC_A2 MAGNETIC -1.0 4.00000E-01 !
PHASE BCC_A2 %& 2 1 3 !
CONSTITUENT BCC_A2 :FE%,NB%,NI : VA% : !

```

```

PARAMETER G(BCC_A2,FE:VA;0) 2.98150E+02 +GHSERFE#;
6.00000E+03 N 1991DINSDA !
PARAMETER TC(BCC_A2,FE:VA;0) 2.98150E+02 1043; 6.00000E+03
N 1991DINSDA !
PARAMETER BMAGN(BCC_A2,FE:VA;0) 2.98150E+02 2.22; 6.00000E+03 N
1991DINSDA !
PARAMETER G(BCC_A2,NB:VA;0) 2.98150E+02 +GHSERNB#; 6.00000E+03 N
1991DINSDA !
PARAMETER TC(BCC_A2,NB:VA;0) 2.98150E+02 +ZEROMU#; 6.00000E+03 N
2008MEMO !
PARAMETER BMAGN(BCC_A2,NB:VA;0) 2.98150E+02 +ZEROMU#; 6.00000E+03 N
2008MEMO !
PARAMETER G(BCC_A2,NI:VA;0) 2.98140E+02 +GNIBCC#; 3.00000E+03 N
1991DINSDA !
PARAMETER TC(BCC_A2,NI:VA;0) 2.98150E+02 575; 6.00000E+03 N
1991DINSDA !
PARAMETER BMAGN(BCC_A2,NI:VA;0) 2.98150E+02 .85; 6.00000E+03 N
1991DINSDA !
PARAMETER G(BCC_A2,FE,NB:VA;0) 2.98150E+02 +16016.944+.00995*T;
6.00000E+03 N 2000TOFFOL !
PARAMETER G(BCC_A2,FE,NB:VA;1) 2.98150E+02 -9737.8048+1.911*T;
6.00000E+03 N 2000TOFFOL !
PARAMETER G(BCC_A2,FE,NB:VA;2) 2.98150E+02 -8392.8109-.0213*T;
6.00000E+03 N 2000TOFFOL !
PARAMETER BMAGN(BCC_A2,FE,NB:VA;0) 2.98150E+02 +ZEROMU#; 6.00000E+03
N 2008MEMO !
PARAMETER TC(BCC_A2,FE,NB:VA;0) 2.98150E+02 +ZEROMU#; 6.00000E+03 N
2008MEMO !
PARAMETER G(BCC_A2,FE,NI:VA;0) 2.98150E+02 -956.63-1.28726*T;

```



```

6.00000E+03    N 1986DINSDA    !
PARAMETER G(BCC_A2,FE,NI:VA;1)  2.98150E+02  +1789.03-1.92912*T;
6.00000E+03    N 1986DINSDA    !
PARAMETER BMAGN(BCC_A2,FE,NI:VA;0)  2.98150E+02  +ZEROMU#;    6.00000E+03
N 2008MEMO    !
PARAMETER TC(BCC_A2,FE,NI:VA;0)  2.98150E+02  +ZEROMU#;    6.00000E+03    N
2008MEMO    !
PARAMETER G(BCC_A2,NB,NI:VA;0)  2.98150E+02  -18724.3+5.02405*T;
6.00000E+03    N 1996BOLCAV    !
PARAMETER BMAGN(BCC_A2,NB,NI:VA;0)  2.98150E+02  +ZEROMU#;    6.00000E+03
N 2008MEMO    !
PARAMETER TC(BCC_A2,NB,NI:VA;0)  2.98150E+02  +ZEROMU#;    6.00000E+03    N
2008MEMO    !
PARAMETER G(BCC_A2,FE,NB,NI:VA;0)  2.98150E+02  +ZEROMU#;    6.00000E+03
N 2008MEMO    !

PHASE C14_LAVES    %    2    2    1    !
CONSTITUENT C14_LAVES    :FE,NB,NI%    :    FE,NB%,NI    :    !

PARAMETER G(C14_LAVES,FE:FE;0)  2.98150E+02  +15000+3*GHSEFE#;
6.00000E+03    N 2000TOFFOL    !
PARAMETER G(C14_LAVES,NB:FE;0)  2.98150E+02  +73200+15000+15000-17.4519*T
+2*GHSEFE#;    6.00000E+03    N 2000TOFFOL    !
PARAMETER G(C14_LAVES,NI:FE;0)  2.98150E+02  +15000+15000-15000
+2*GHSEFE#;    6.00000E+03    N 2008MEMO    !
PARAMETER G(C14_LAVES,FE:NB;0)  2.98150E+02  -73200+17.4519*T+2*GHSEFE#
+GHSEFE#;    6.00000E+03    N 2000TOFFOL    !
PARAMETER G(C14_LAVES,NB:NB;0)  2.98150E+02  +15000+3*GHSEFE#;
6.00000E+03    N 1993COSTA    !
PARAMETER G(C14_LAVES,NI:NB;0)  2.98150E+02  -73200+17.4519*T+2*GHSEFE#
+GHSEFE#;    6.00000E+03    N 2008MEMO    !
PARAMETER G(C14_LAVES,FE:NI;0)  2.98150E+02  +15000+2*GHSEFE#+GHSEFE#;
6.00000E+03    N 2008MEMO    !
PARAMETER G(C14_LAVES,NB:NI;0)  2.98150E+02  +15000+15000+73200-17.4519*T
+2*GHSEFE#+GHSEFE#;    6.00000E+03    N 2008MEMO    !
PARAMETER G(C14_LAVES,NI:NI;0)  2.98150E+02  +15000+3*GHSEFE#;
6.00000E+03    N 1995DUPIN    !
PARAMETER G(C14_LAVES,FE,NB:FE;0)  2.98150E+02  +114+44.2245*T;
6.00000E+03    N 2000TOFFOL    !
PARAMETER G(C14_LAVES,FE,NI:FE;0)  2.98150E+02  +ZEROMU#;    6.00000E+03
N 2008MEMO    !
PARAMETER G(C14_LAVES,FE:FE,NB;0)  2.98150E+02  -2381.4096+13.9221*T;
6.00000E+03    N 2000TOFFOL    !
PARAMETER G(C14_LAVES,FE:FE,NI;0)  2.98150E+02  +ZEROMU#;    6.00000E+03
N 2008MEMO    !
PARAMETER G(C14_LAVES,NB,NI:FE;0)  2.98150E+02  +114+44.2245*T;
6.00000E+03    N 2008MEMO    !
PARAMETER G(C14_LAVES,NB:FE,NB;0)  2.98150E+02  -2381.4096+13.9221*T;
6.00000E+03    N 2000TOFFOL    !
PARAMETER G(C14_LAVES,NB:FE,NI;0)  2.98150E+02  +ZEROMU#;    6.00000E+03
N 2008MEMO    !
PARAMETER G(C14_LAVES,NI:FE,NI;0)  2.98150E+02  +ZEROMU#;    6.00000E+03
N 2008MEMO    !
PARAMETER G(C14_LAVES,NI:FE,NB;0)  2.98150E+02  -2381.4096+13.9221*T;
6.00000E+03    N 2008MEMO    !
PARAMETER G(C14_LAVES,FE,NB:NB;0)  2.98150E+02  +114+44.2245*T;
6.00000E+03    N 2000TOFFOL    !
PARAMETER G(C14_LAVES,FE,NI:NB;0)  2.98150E+02  +21280.15-48.31979*T;
6.00000E+03    N 2008MEMO    !
PARAMETER G(C14_LAVES,FE:NB,NI;0)  2.98150E+02  -2381.4096+13.9221*T;
6.00000E+03    N 2008MEMO    !

```

```

PARAMETER G(C14_LAVES,NB,NI:NB;0) 2.98150E+02 +114+44.2245*T;
6.00000E+03 N 2008MEMO !
PARAMETER G(C14_LAVES,NB:NB,NI;0) 2.98150E+02 -2381.4096+13.9221*T;
6.00000E+03 N 2008MEMO !
PARAMETER G(C14_LAVES,NI:NB,NI;0) 2.98150E+02 -2381.4096+13.9221*T;
6.00000E+03 N 2008MEMO !
PARAMETER G(C14_LAVES,FE,NI:NI;0) 2.98150E+02 +ZEROMU#; 6.00000E+03
N 2008MEMO !
PARAMETER G(C14_LAVES,FE,NB:NI;0) 2.98150E+02 +114+44.2245*T;
6.00000E+03 N 2008MEMO !
PARAMETER G(C14_LAVES,NB,NI:NI;0) 2.98150E+02 +114+44.2245*T;
6.00000E+03 N 2008MEMO !
PARAMETER G(C14_LAVES,FE,NB,NI:*;0) 2.98150E+02 +ZEROMU#; 6.00000E+03
N 2008MEMO !
PARAMETER G(C14_LAVES,*:FE,NB,NI;0) 2.98150E+02 +ZEROMU#; 6.00000E+03
N 2008MEMO !

PHASE C15_LAVES % 2 2 1 !
CONSTITUENT C15_LAVES :FE,NB,NI% : FE,NB%,NI : !

PARAMETER G(C15_LAVES,FE:FE;0) 2.98150E+02 +15000+3*GHSEFE#;
6.00000E+03 N 2008MEMO !
PARAMETER G(C15_LAVES,NB:FE;0) 2.98150E+02 +15000+15000+67686.5
-22.2*T+GHSEFE#+2*GHSENB#; 6.00000E+03 N 2008MEMO !
PARAMETER G(C15_LAVES,NI:FE;0) 2.98150E+02 +15000+15000-15000
+2*GHSENI#+GHSEFE#; 6.00000E+03 N 2008MEMO !
PARAMETER G(C15_LAVES,FE:NB;0) 2.98150E+02 -67686.5+22.2*T
+2*GHSEFE#+GHSENB#; 6.00000E+03 N 2008MEMO !
PARAMETER G(C15_LAVES,NB:NB;0) 2.98150E+02 +15000+3*GHSENB#;
6.00000E+03 N 1993COSTA !
PARAMETER G(C15_LAVES,NI:NB;0) 2.98150E+02 -67686.5+22.2*T
+2*GHSENI#+GHSENB#; 6.00000E+03 N 2008MEMO !
PARAMETER G(C15_LAVES,FE:NI;0) 2.98150E+02 +15000+2*GHSEFE#+GHSENI#;
6.00000E+03 N 2008MEMO !
PARAMETER G(C15_LAVES,NB:NI;0) 2.98150E+02 +15000+15000+67686.5
-22.2*T+2*GHSENB#+GHSENI#; 6.00000E+03 N 2008MEMO !
PARAMETER G(C15_LAVES,NI:NI;0) 2.98150E+02 +15000+3*GHSENI#;
6.00000E+03 N 1995DUPIN !
PARAMETER G(C15_LAVES,FE,NB:FE;0) 2.98150E+02 83366.02; 6.00000E+03
N 2008MEMO !
PARAMETER G(C15_LAVES,FE,NI:FE;0) 2.98150E+02 +ZEROMU#; 6.00000E+03
N 2008MEMO !
PARAMETER G(C15_LAVES,FE:FE,NB;0) 2.98150E+02 17565.57; 6.00000E+03
N 2008MEMO !
PARAMETER G(C15_LAVES,FE:FE,NI;0) 2.98150E+02 +ZEROMU#; 6.00000E+03
N 2008MEMO !
PARAMETER G(C15_LAVES,NB,NI:FE;0) 2.98150E+02 83366.02; 6.00000E+03
N 2008MEMO !
PARAMETER G(C15_LAVES,NB:FE,NB;0) 2.98150E+02 17565.57; 6.00000E+03
N 2008MEMO !
PARAMETER G(C15_LAVES,NB:FE,NI;0) 2.98150E+02 +ZEROMU#; 6.00000E+03
N 2008MEMO !
PARAMETER G(C15_LAVES,NI:FE,NI;0) 2.98150E+02 +ZEROMU#; 6.00000E+03
N 2008MEMO !
PARAMETER G(C15_LAVES,NI:FE,NB;0) 2.98150E+02 17565.57; 6.00000E+03
N 2008MEMO !
PARAMETER G(C15_LAVES,FE,NB:NB;0) 2.98150E+02 83366.02; 6.00000E+03
N 2008MEMO !
PARAMETER G(C15_LAVES,FE,NI:NB;0) 2.98150E+02 +ZEROMU#; 6.00000E+03
N 2008MEMO !
PARAMETER G(C15_LAVES,FE:NB,NI;0) 2.98150E+02 17565.57; 6.00000E+03

```



```

N 2008MEMO      !
PARAMETER G(C15_LAVES,NB,NI:NB;0)  2.98150E+02  83366.02;    6.00000E+03
N 2008MEMO      !
PARAMETER G(C15_LAVES,NB:NB,NI;0)  2.98150E+02  17565.57;    6.00000E+03
N 2008MEMO      !
PARAMETER G(C15_LAVES,NI:NB,NI;0)  2.98150E+02  17565.57;    6.00000E+03
N 2008MEMO      !
PARAMETER G(C15_LAVES,FE,NI:NI;0)  2.98150E+02  +ZEROMU#;    6.00000E+03
N 2008MEMO      !
PARAMETER G(C15_LAVES,FE,NB:NI;0)  2.98150E+02  83366.02;    6.00000E+03
N 2008MEMO      !
PARAMETER G(C15_LAVES,NB,NI:NI;0)  2.98150E+02  83366.02;    6.00000E+03
N 2008MEMO      !
PARAMETER G(C15_LAVES,FE,NB,NI:*;0)  2.98150E+02  +ZEROMU#;    6.00000E+03
N 2008MEMO      !
PARAMETER G(C15_LAVES,*:FE,NB,NI;0)  2.98150E+02  +ZEROMU#;    6.00000E+03
N 2008MEMO      !

```

```

PHASE D022_NBNI3  %  2 1  3 !
CONSTITUENT D022_NBNI3  :FE,NB%,NI : FE,NB,NI% :  !

```

```

PARAMETER G(D022_NBNI3,FE:FE;0)  2.98150E+02  20000+4*GHSEFE#;
6.00000E+03  N 2008MEMO      !
PARAMETER G(D022_NBNI3,NB:FE;0)  2.98150E+02  -54000+25*T
+GHSEFE#; 6.00000E+03  N 2008MEMO      !
PARAMETER G(D022_NBNI3,NI:FE;0)  2.98150E+02  20000+GHSEFE#;
6.00000E+03  N 2008MEMO      !
PARAMETER G(D022_NBNI3,FE:NB;0)  2.98150E+02  20000+20000
+54000-25*T+GHSEFE#; 6.00000E+03  N 2008MEMO      !
PARAMETER G(D022_NBNI3,NB:NB;0)  2.98150E+02  20000+4*GHSEFE#;
6.00000E+03  N 2008MEMO      !
PARAMETER G(D022_NBNI3,NI:NB;0)  2.98150E+02  20000+20000
+62000+GHSEFE#; 6.00000E+03  N 2008MEMO      !
PARAMETER G(D022_NBNI3,FE:NI;0)  2.98150E+02  20000+20000
-20000+GHSEFE#; 6.00000E+03  N 2008MEMO      !
PARAMETER G(D022_NBNI3,NB:NI;0)  2.98150E+02  -62000+GHSEFE#;
6.00000E+03  N 2008MEMO      !
PARAMETER G(D022_NBNI3,NI:NI;0)  2.98150E+02  20000+4*GHSEFE#;
6.00000E+03  N 2008MEMO      !

```

```

PHASE D0A_NBNI3  %  2 1  3 !
CONSTITUENT D0A_NBNI3  :FE,NB%,NI : FE,NB,NI% :  !

```

```

PARAMETER G(D0A_NBNI3,FE:FE;0)  2.98150E+02  +20000+4*GHSEFE#;
6.00000E+03  N 2008MEMO      !
PARAMETER G(D0A_NBNI3,NB:FE;0)  2.98150E+02  -8500+25*T
+GHSEFE#; 6.00000E+03  N 2008MEMO      !
PARAMETER G(D0A_NBNI3,NI:FE;0)  2.98150E+02  +20000+20000-20000+GHSEFE#;
6.00000E+03  N 2008MEMO      !
PARAMETER G(D0A_NBNI3,FE:NB;0)  2.98150E+02  +20000+20000+8500-25*T
+GHSEFE#; 6.00000E+03  N 2008MEMO      !
PARAMETER G(D0A_NBNI3,NB:NB;0)  2.98150E+02  +20000+4*GHSEFE#;
6.00000E+03  N 1996BOLCAV      !
PARAMETER G(D0A_NBNI3,NI:NB;0)  2.98150E+02  +181202.3-19.33288*T
+GHSEFE#; 6.00000E+03  N 1996BOLCAV      !
PARAMETER G(D0A_NBNI3,FE:NI;0)  2.98150E+02  +20000+GHSEFE#;
6.00000E+03  N 2008MEMO      !
PARAMETER G(D0A_NBNI3,NB:NI;0)  2.98150E+02  -141202.4+19.33288*T
+GHSEFE#; 6.00000E+03  N 1996BOLCAV      !
PARAMETER G(D0A_NBNI3,NI:NI;0)  2.98150E+02  +20000+4*GHSEFE#;
6.00000E+03  N 1996BOLCAV      !

```

```

PARAMETER G(D0A_NBNI3,FE,NB:FE;0) 2.98150E+02 -12318.5; 6.00000E+03
N 2008MEMO !
PARAMETER G(D0A_NBNI3,FE,NI:FE;0) 2.98150E+02 +ZEROMU#; 6.00000E+03
N 2008MEMO !
PARAMETER G(D0A_NBNI3,FE:FE,NB;0) 2.98150E+02 54022.5; 6.00000E+03
N 2008MEMO !
PARAMETER G(D0A_NBNI3,FE:FE,NI;0) 2.98150E+02 +ZEROMU#; 6.00000E+03
N 2008MEMO !
PARAMETER G(D0A_NBNI3,NB,NI:FE;0) 2.98150E+02 -12318.5; 6.00000E+03
N 2008MEMO !
PARAMETER G(D0A_NBNI3,NB:FE,NB;0) 2.98150E+02 54022.5; 6.00000E+03
N 2008MEMO !
PARAMETER G(D0A_NBNI3,NB:FE,NI;0) 2.98150E+02 +ZEROMU#; 6.00000E+03
N 2008MEMO !
PARAMETER G(D0A_NBNI3,NI:FE,NI;0) 2.98150E+02 +ZEROMU#; 6.00000E+03
N 2008MEMO !
PARAMETER G(D0A_NBNI3,NI:FE,NB;0) 2.98150E+02 54022.5; 6.00000E+03
N 2008MEMO !
PARAMETER G(D0A_NBNI3,FE,NB:NB;0) 2.98150E+02 -12318.5; 6.00000E+03
N 2008MEMO !
PARAMETER G(D0A_NBNI3,FE,NI:NB;0) 2.98150E+02 +ZEROMU#; 6.00000E+03
N 2008MEMO !
PARAMETER G(D0A_NBNI3,FE:NB,NI;0) 2.98150E+02 54022.5; 6.00000E+03
N 2008MEMO !
PARAMETER G(D0A_NBNI3,NB,NI:NB;0) 2.98150E+02 -12318.5; 6.00000E+03
N 1996BOLCAV !
PARAMETER G(D0A_NBNI3,NB:NB,NI;0) 2.98150E+02 54022.5; 6.00000E+03
N 1996BOLCAV !
PARAMETER G(D0A_NBNI3,NI:NB,NI;0) 2.98150E+02 54022.5; 6.00000E+03
N 1996BOLCAV !
PARAMETER G(D0A_NBNI3,FE,NI:NI;0) 2.98150E+02 +ZEROMU#; 6.00000E+03
N 2008MEMO !
PARAMETER G(D0A_NBNI3,FE,NB:NI;0) 2.98150E+02 -33275.97; 6.00000E+03
N 2008MEMO !
PARAMETER G(D0A_NBNI3,NB,NI:NI;0) 2.98150E+02 -12318.5; 6.00000E+03
N 1996BOLCAV !
PARAMETER G(D0A_NBNI3,FE,NB,NI:*;0) 2.98150E+02 +ZEROMU#; 6.00000E+03
N 2008MEMO !
PARAMETER G(D0A_NBNI3,*:FE,NB,NI;0) 2.98150E+02 +ZEROMU#; 6.00000E+03
N 2008MEMO !

```

PHASE D85\_NI7NB6 % 2 6 7 !

CONSTITUENT D85\_NI7NB6 :NB : FE,NB,NI% : !

```

PARAMETER G(D85_NI7NB6,NB:FE;0) 2.98150E+02 -305500+81.653*T+7*GFEFCC#
+6*GHSERNB#; 6.00000E+03 N 2000TOFFOL !
PARAMETER G(D85_NI7NB6,NB:NB;0) 2.98150E+02 +65000+13*GHSERNB#;
6.00000E+03 N 1996BOLCAV !
PARAMETER G(D85_NI7NB6,NB:NI;0) 2.98150E+02 -312097.5+7.3203*T
+6*GHSERNB#+7*GHSERNI#; 6.00000E+03 N 1996BOLCAV !
PARAMETER G(D85_NI7NB6,NB:FE,NB;0) 2.98150E+02 +175000+50*T;
6.00000E+03 N 2008MEMO !
PARAMETER G(D85_NI7NB6,NB:FE,NB;1) 2.98150E+02 -69960; 6.00000E+03
N 2008MEMO !
PARAMETER G(D85_NI7NB6,NB:FE,NI;0) 2.98150E+02 +ZEROMU#; 6.00000E+03
N 2008MEMO !
PARAMETER G(D85_NI7NB6,NB:NB,NI;0) 2.98150E+02 273734.5; 6.00000E+03
N 1996BOLCAV !
PARAMETER G(D85_NI7NB6,NB:NB,NI;1) 2.98150E+02 451218.3; 6.00000E+03
N 1996BOLCAV !
PARAMETER G(D85_NI7NB6,NB:FE,NB,NI;0) 2.98150E+02 +ZEROMU#;

```



```

6.00000E+03    N 2008MEMO    !

TYPE_DEFINITION ' GES A_P_D FCC_A1 MAGNETIC -3.0    2.80000E-01 !
PHASE FCC_A1 '%' 2 1 1 !
CONSTITUENT FCC_A1 :FE%,NB,NI% : VA% : !

PARAMETER G(FCC_A1,FE:VA;0) 2.98150E+02 +GFEFCC#+GPFEFCC#;
6.00000E+03    N 1991DINSDA !
PARAMETER TC(FCC_A1,FE:VA;0) 2.98150E+02 -201; 6.00000E+03    N
1991DINSDA !
PARAMETER BMAGN(FCC_A1,FE:VA;0) 2.98150E+02 -2.1; 6.00000E+03    N
1991DINSDA !
PARAMETER G(FCC_A1,NB:VA;0) 2.98150E+02 +13500+1.7*T+GHEXTNB#;
6.00000E+03    N 1991DINSDA !
PARAMETER TC(FCC_A1,NB:VA;0) 2.98150E+02 +ZEROMU#; 6.00000E+03    N
2008MEMO !
PARAMETER BMAGN(FCC_A1,NB:VA;0) 2.98150E+02 +ZEROMU#; 6.00000E+03    N
2008MEMO !
PARAMETER G(FCC_A1,NI:VA;0) 2.98140E+02 +GHSERNI#; 3.00000E+03    N
1991DINSDA !
PARAMETER TC(FCC_A1,NI:VA;0) 2.98150E+02 633; 6.00000E+03    N
1991DINSDA !
PARAMETER BMAGN(FCC_A1,NI:VA;0) 2.98150E+02 .52; 6.00000E+03    N
1991DINSDA !
PARAMETER G(FCC_A1,FE,NB:VA;0) 2.98150E+02 +2651.9737-8.0597*T;
6.00000E+03    N 2000TOFFOL !
PARAMETER TC(FCC_A1,FE,NB:VA;0) 2.98150E+02 +ZEROMU#; 6.00000E+03    N
2008MEMO !
PARAMETER BMAGN(FCC_A1,FE,NB:VA;0) 2.98150E+02 +ZEROMU#; 6.00000E+03
N 2008MEMO !
PARAMETER G(FCC_A1,FE,NI:VA;0) 2.98150E+02 -12054.355+3.27413*T;
6.00000E+03    N 1986DINSDA !
PARAMETER G(FCC_A1,FE,NI:VA;1) 2.98150E+02 +11082.1315-4.45077*T;
6.00000E+03    N 1986DINSDA !
PARAMETER G(FCC_A1,FE,NI:VA;2) 2.98150E+02 -725.805174; 6.00000E+03
N 1986DINSDA !
PARAMETER TC(FCC_A1,FE,NI:VA;0) 2.98150E+02 2133; 6.00000E+03    N
1986DINSDA !
PARAMETER TC(FCC_A1,FE,NI:VA;1) 2.98150E+02 -682; 6.00000E+03    N
1986DINSDA !
PARAMETER BMAGN(FCC_A1,FE,NI:VA;0) 2.98150E+02 9.55; 6.00000E+03    N
1986DINSDA !
PARAMETER BMAGN(FCC_A1,FE,NI:VA;1) 2.98150E+02 7.23; 6.00000E+03    N
1986DINSDA !
PARAMETER BMAGN(FCC_A1,FE,NI:VA;2) 2.98150E+02 5.93; 6.00000E+03    N
1986DINSDA !
PARAMETER BMAGN(FCC_A1,FE,NI:VA;3) 2.98150E+02 6.18; 6.00000E+03    N
1986DINSDA !
PARAMETER G(FCC_A1,NB,NI:VA;0) 2.98150E+02 -70007.4-7.39665*T;
6.00000E+03    N 1996BOLCAV !
PARAMETER G(FCC_A1,NB,NI:VA;1) 2.98150E+02 +96115-23.07497*T;
6.00000E+03    N 1996BOLCAV !
PARAMETER TC(FCC_A1,NB,NI:VA;0) 2.98150E+02 -1200; 6.00000E+03    N
1996BOLCAV !
PARAMETER TC(FCC_A1,NB,NI:VA;1) 2.98150E+02 760; 6.00000E+03    N
1996BOLCAV !
PARAMETER BMAGN(FCC_A1,NB,NI:VA;0) 2.98150E+02 +ZEROMU#; 6.00000E+03
N 1996BOLCAV !
PARAMETER BMAGN(FCC_A1,NB,NI:VA;1) 2.98150E+02 +ZEROMU#; 6.00000E+03
N 1996BOLCAV !
PARAMETER G(FCC_A1,FE,NB,NI:VA;0) 2.98150E+02 +ZEROMU#; 6.00000E+03

```

```

N 2008MEMO      !

$ THIS PHASE HAS A DISORDERED CONTRIBUTION FROM FCC_A1
TYPE_DEFINITION ( GES AMEND_PHASE_DESCRIPTION L12_FCC DIS_PART FCC_A1,,, !
PHASE L12_FCC  %( 3 .75 .25 1 !
    CONSTITUENT L12_FCC :FE,NB,NI% : FE,NB%,NI : VA :      !

PARA G(L12_FCC,FE:FE:VA;0) 298.15 0; 6000 N!
PARAMETER G(L12_FCC,NB:FE:VA;0) 2.98150E+02 +3*FENBMEMO#; 6.00000E+03
N 2008MEMO      !
PARAMETER G(L12_FCC,NI:FE:VA;0) 2.98150E+02 +ANGFENI3#; 6.00000E+03
N 2000ANSARA    !
PARAMETER G(L12_FCC,FE:NB:VA;0) 2.98150E+02 +3*FENBMEMO#; 6.00000E+03
N 2008MEMO      !
PARA G(L12_FCC,NB:NB:VA;0) 298.15 0; 6000 N!
PARAMETER G(L12_FCC,NI:NB:VA;0) 2.98150E+02 +3*U1NBNIDU#; 6.00000E+03
N 2003DU        !
PARAMETER G(L12_FCC,FE:NI:VA;0) 2.98150E+02 +ANGFE3NI#; 6.00000E+03
N 2000ANSARA    !
PARAMETER G(L12_FCC,NB:NI:VA;0) 2.98150E+02 +3*U1NBNIDU#; 6.00000E+03
N 2003DU        !
PARA G(L12_FCC,NI:NI:VA;0) 298.15 0; 6000 N!
PARAMETER G(L12_FCC,FE,NB:FE:VA;0) 2.98150E+02 +6*FENBMEMO#;
6.00000E+03 N 2008MEMO      !
PARAMETER G(L12_FCC,FE,NB:NB:VA;0) 2.98150E+02 +6*FENBMEMO#;
6.00000E+03 N 2008MEMO      !
PARAMETER G(L12_FCC,FE:FE,NB:VA;0) 2.98150E+02 +ZEROMU#; 6.00000E+03
N 2008MEMO      !
PARAMETER G(L12_FCC,NB:FE,NB:VA;0) 2.98150E+02 +ZEROMU#; 6.00000E+03
N 2008MEMO      !
PARAMETER G(L12_FCC,FE,NI:FE:VA;0) 2.98150E+02 -1.5*ANGFENI3#
+1.5*AGFE2NI2#+1.5*ANGFE3NI#+3*ANUFENI#; 6.00000E+03 N 2008MEMO      !
PARAMETER G(L12_FCC,FE,NI:FE:VA;1) 2.98150E+02 +.5*ANGFENI3#
-1.5*AGFE2NI2#+1.5*ANGFE3NI#; 6.00000E+03 N 2008MEMO      !
PARAMETER G(L12_FCC,FE,NI:NI:VA;0) 2.98150E+02 +1.5*ANGFENI3#
+1.5*AGFE2NI2#-1.5*ANGFE3NI#+3*ANUFENI#; 6.00000E+03 N 2008MEMO      !
PARAMETER G(L12_FCC,FE,NI:NI:VA;1) 2.98150E+02 -1.5*ANGFENI3#
+1.5*AGFE2NI2#-.5*ANGFE3NI#; 6.00000E+03 N 2008MEMO      !
PARAMETER G(L12_FCC,FE:FE,NI:VA;0) 2.98150E+02 +ANUFENI#; 6.00000E+03
N 2008MEMO      !
PARAMETER G(L12_FCC,NI:FE,NI:VA;0) 2.98150E+02 +ANUFENI#; 6.00000E+03
N 2008MEMO      !
PARAMETER G(L12_FCC,NB,NI:NB:VA;0) 2.98150E+02 +6*U1NBNIDU#;
6.00000E+03 N 2003DU        !
PARAMETER G(L12_FCC,NB,NI:NI:VA;0) 2.98150E+02 +6*U1NBNIDU#;
6.00000E+03 N 2003DU        !
PARAMETER G(L12_FCC,NB:NB,NI:VA;0) 2.98150E+02 +ZEROMU#; 6.00000E+03
N 2003DU        !
PARAMETER G(L12_FCC,NI:NB,NI:VA;0) 2.98150E+02 +ZEROMU#; 6.00000E+03
N 2003DU        !

PARAMETER G(L12_FCC,FE,NB:NI:VA;0) 2.98150E+02 +ZEROMU#+1.5*FE2NBNIM#
+1.5*FENB2NIM#-1.5*NB3NIM#-1.5*FE3NIM#; 6.00000E+03 N 2008MEMO      !
PARAMETER G(L12_FCC,FE,NB:NI:VA;1) 2.98150E+02 +ZEROMU#+1.5*FE2NBNIM#
-1.5*FENB2NIM#+.5*NB3NIM#-.5*FE3NIM#; 6.00000E+03 N 2008MEMO      !
PARAMETER G(L12_FCC,NB,NI:FE:VA;0) 2.98150E+02 +ZEROMU#+1.5*FENB2NIM#
+1.5*FENBNI2M#-1.5*FENI3M#-1.5*FENB3M#; 6.00000E+03 N 2008MEMO      !
PARAMETER G(L12_FCC,NB,NI:FE:VA;1) 2.98150E+02 +ZEROMU#+1.5*FENB2NIM#
-1.5*FENBNI2M#+.5*FENI3M#-.5*FENB3M#; 6.00000E+03 N 2008MEMO      !
PARAMETER G(L12_FCC,FE,NI:NB:VA;0) 2.98150E+02 +ZEROMU#+1.5*FE2NBNIM#
+1.5*FENBNI2M#-1.5*NBNI3M#-1.5*FE3NBM#+3*ANUFENI#; 6.00000E+03 N

```



```

2008MEMO      !
PARAMETER G(L12_FCC,FE,NI:NB:VA;1)  2.98150E+02  +ZEROMU#+1.5*FE2NBNIM#
-1.5*FENBNI2M#+.5*NBNI3M#-.5*FE3NBM#;    6.00000E+03  N 2008MEMO      !
PARAMETER G(L12_FCC,FE:NB,NI:VA;0)  2.98150E+02  +ZEROMU#;    6.00000E+03
N 2008MEMO      !
PARAMETER G(L12_FCC,NI:FE,NB:VA;0)  2.98150E+02  +ZEROMU#;    6.00000E+03
N 2008MEMO      !
PARAMETER G(L12_FCC,NB:FE,NI:VA;0)  2.98150E+02  +ANUFENI#;    6.00000E+03
N 2008MEMO      !
PARAMETER G(L12_FCC,FE,NB,NI:FE:VA;0)  2.98150E+02  +6*FE2NBNIM#
-1.5*FENB2NIM#-1.5*FENBNI2M#-1.5*FE3NBM#-1.5*FE2NB2M#+FENB3M#-1.5*FE3NIM#
-1.5*FE2NI2M#+FENI3M#;    6.00000E+03  N 2008MEMO      !
PARAMETER G(L12_FCC,FE,NB,NI:NB:VA;0)  2.98150E+02  +6*FENB2NIM#
-1.5*FE2NBNIM#-1.5*FENBNI2M#-1.5*FENB3M#-1.5*FE2NB2M#+FE3NBM#-1.5*NB3NIM#
-1.5*NB2NI2M#+NBNI3M#;    6.00000E+03  N 2008MEMO      !
PARAMETER G(L12_FCC,FE,NB,NI:NI:VA;0)  2.98150E+02  +6*FENBNI2M#
-1.5*FE2NBNIM#-1.5*FENB2NIM#-1.5*FENI3M#-1.5*FE2NI2M#+FE3NIM#-1.5*NBNI3M#
-1.5*NB2NI2M#+NB3NIM#;    6.00000E+03  N 2008MEMO      !
PARAMETER G(L12_FCC,FE:FE,NB,NI:VA;0)  2.98150E+02  +ZEROMU#;    6.00000E+03
N 2008MEMO      !
PARAMETER G(L12_FCC,NB:FE,NB,NI:VA;0)  2.98150E+02  +ZEROMU#;    6.00000E+03
N 2008MEMO      !
PARAMETER G(L12_FCC,NI:FE,NB,NI:VA;0)  2.98150E+02  +ZEROMU#;    6.00000E+03
N 2008MEMO      !

```

#### LIST\_OF\_REFERENCES NUMBER SOURCE

```

1991DINSDA ' SSOL283,NIST191DIN Alan Dinsdale, Calphad Vol 15 (1991) p 317
-425, also in NPL Report DMA(A)195 Rev. August 1990; unaries'
2000TOFFOL ' C. Toffolon and C. Servant, Calphad, (2000), Vol. 24, No 2,
pp. 97-112; FE-NB'
2008MEMO ' THIS WORK, M. MATHON, (2008)'
1993LEE ' B.-J. Lee; Calphad, (1993), 17, 3, pp 251-268 ; FE-CR FE-NI'
1996BOLCAV ' A. Bolcavage, U. R. Kattner, J. Phase equilibria 17 (1996) 92-
100; CR-NB'
1986DINSDA ' SSOL158 and SSOL162, A. Dinsdale, T. Chart, MTDS NPL,
unpublished works (1986); FE-NI'
1993COST ' J. G Costa Neto, S.G. Fries, H. L. Lukas, S. Gama, G. Effenberg,
Calphad 17 (1993) 219-228; CR-NB'
1995DUPIN ' NIST195Dup, N. Dupin, Ph.D. Thesis, LTPCM Grenoble, 1995; Al-
Co,Al-Co-Ni, Al-Cr-Ni, Al-Ni-Ta, Al-Ni-Ti, Cr-Ni-Ta, Cr-Ni-Ti'
2000ANSARA ' Ansara I., Private communication, (2000)'
2003DU ' Du Y., Chang Y. A. Gong W., Huang B., Xu H., Jin Z., Zhang F.
and Chen S.-L., Intermetallics, (2003), 11, 995-1013'
!

```

## References

- [1] Thermo-Calc Software AB, Stockholm Technology Park, Stockholm, Sweden. <http://www.thermocalc.se/>.
- [2] MICRESS, MICROstructure Evolution Simulation Software ACCESS, Aachen University of Technology (RWTH), Aachen, Germany. <http://www.accessMietineerwth-aachen.de/MICRESS/>.
- [3] V. Raghavan, Phase Diagrams Ternary Iron Alloys 2 (1992) 1025–1027.
- [4] V. Raghavan, JPEDAV 25 (2004) 552.
- [5] V. Raghavan, JPEDAV 28 (2007) 389–390.
- [6] V.V. Savin, Fizika Metallov i Metallovedenie 68 (1) (1989) 143–149.
- [7] M. Takeyama, S. Morita, A. Yamauchi, M. Yamanaka, T. Matsuo, in: E.A. Loria (Ed.), Superalloys 718, 625, 706 and Various Derivatives, T.M.S. (The Minerals, Metals and Materials Society), 2001, pp. 333–344.
- [8] M. Takeyama, N. Gomi, S. Morita, T. Matsuo, Mater. Res. Soc. Symp. Proc., 842, 2005, pp. 461–466.
- [9] J. Manenc, J. Bourgeot, H. De Boer, Scripta Metall. 2 (1968) 453–458.
- [10] I. Kirman, Scripta Metall. 2 (1968) 679–680.
- [11] J. Manenc, Scripta Metall. 2 (1968) 705–706.
- [12] W.E. Quist, R. Taggart, D.H. Polonis, Metall. Trans. 2 (1971) 825–832.
- [13] A. Dinsdale, SGTE data for pure elements, CALPHAD 15 (1991) 317–425.
- [14] N. Dupin, I. Ansara, J. Phase Equilib. 14 (4) (1993) 451–456.
- [15] G.C. Coelho, S.G. Fries, H.L. Lukas, P. Majewski, J.M. Zelaya Bejarano, S. Gamma, C.A. Ribeiro, G. Effenberg, Klaus Schulze Symp. Process. Appl., High Purity Refract. Met. Alloys, Proc. Symp. Meeting in 1993, 1994, pp. 51–70.
- [16] A. Dinsdale, T. Chart, MTDS NPL, 1986, Unpublished work.
- [17] A. Bolcavage, U.R. Kattner, J. Phase Equilibria 17 (1996) 92–100.
- [18] W. Huang, Z. Metallkd. 81 (1990) 397–404.
- [19] J.M. Zelaya Bejarano, S. Gamma, C.A. Ribeiro, Effenberg, Z. Metallkd. 84 (1993) 160–164.
- [20] S. Srikanth, A. Petric, Z. Metallkd. 85 (3) (1994) 164–170.
- [21] J.G. Costa Neto, S.G. Fries, H.L. Lukas, S. Gama, G. Effenberg, CALPHAD 17 (1993) 219–228.
- [22] M. Mathon, CIRIMAT, 2008, Unpublished work on Cr–Fe–Nb–Ni; Muriel Mathon, Damien Connétable, Jacques Lacaze, Juliette Huez, Bo Sundman, Calphad-type assessment of the Cr–Fe–Nb–Ni quaternary system (poster), in: Calphad XXXVII Conference, 15–20 June 2008.
- [23] C. Toffolon, C. Servant, Calphad 24 (2) (2000) 97–112.
- [24] D.A. Read, G.C. Hallam, M.S. Sabota, A. Mustaffa, Physica B 86–88 (1977) 66–68.

- [25] L.V. Osipova, L.A. Panteleimonov, *Izv. Akad. Nauk. SSSR. Met.* 3 (1982) 205–206.
- [26] M. Shiga, Y. Nakamura, *J. Phys. Soc. Japan* 56 (1987) 4040–4046.
- [27] J. Inoue, M. Shimizu, *J. Magn. Magn. Mater.* 79 (2) (1989) 265–269.
- [28] Y. Yamada, H. Nakamura, Y. Kitakao, K. Asayama, K. Koga, A. Sakata, *J. Phys. Soc. Japan* 59 (1990) 2976.
- [29] Y. Yamada, R. Moru, K. Hirano, T. Hirotsuji, G. Obara, T. Nakamura, *J. Magn. Magn. Mater.* 310 (2007) 1812–1814.
- [30] R. Sato Turtelli, J.P. Sinnecker, R. Grössinger, A. Penton-Madrigal, E. Estevez-Rams, *J. Magn. Magn. Mater.* 316 (2007) e492–e495.
- [31] M.R. Crook, R. Cywinski, *J. Magn. Magn. Mater.* 140–144 (1995) 71–72.
- [32] M. Kobayashi, T. Kai, N. Takano, Y. Ohashi, K. Shiiki, *J. Magn. Magn. Mater.* 166 (1997) 329–333.
- [33] Z.S. Xing, D.D. Gohil, A. Dinsdale, T. Chart, *DMA (A)* 103, National Physical Laboratory, London, 1985.
- [34] A. Gabriel, P. Gustafsson, I. Ansara, *CALPHAD* 11 (1987) 203–218.
- [35] B.-J. Lee, *CALPHAD* 17 (3) (1993) 251–268.
- [36] J. Miettinen, *CALPHAD* 23 (2) (1999) 231–248.
- [37] J. Miettinen, Unpublished work on Cr–Fe–Ni–B, 2007.
- [38] I. Ohnuma, R. Kainuma, K. Ishida, *Calphad and alloy thermodynamics*, in: *Proceedings of a Symposium Held During the TMS Annual Meeting Seattle, WA, US, February 17–21, 2002*, pp. 61–78.
- [39] C.W. Yang, D.B. Williams, J.I. Goldstein, *J. Phase Equilib.* 17 (6) (1996) 522.
- [40] C.W. Yang, D.B. Williams, J.I. Goldstein, *Geochim. Cosmochim. Acta* 61 (14) (1997) 2943–2956.
- [41] Z. Kejun, Z. Xianzhang, J. Zhanpeng, *J. Alloy Compd.* 179 (1–2) (1992) 177–185.
- [42] H. Chen, Y. Du, *CALPHAD* 30 (2006) 308–315.
- [43] L.M. Joubert, B. Sundman, N. Dupin, *CALPHAD* 28 (2004) 299–306.
- [44] Z.I. Ali-Zade, T.M. Panakhov, A.I. Ibraginov, *Thermodyn. Svoist. Metal. Splav.* 56 (1975) 218–221.
- [45] T. Fangt, S.J. Kennedy, L. Quan, T.J. Hicks, *J. Phys. Condens. Matter.* 4 (1992) 2405–2414.
- [46] P. Ravindran, G. Subramoniam, R. Asokamani, *Phys. Rev. B* 53 (3) (1996) 1129–1137.
- [47] NRL, Materials Science and Technology Division, Code 6300, Naval Research Laboratory, Washington, DC 20375, USA. <http://cst-www.nrl.navy.mil/lattice/index.html>.
- [48] K. Mitsuoka, H. Miyajima, H. Ino, S. Chikazumi, *J. Phys. Soc. Japan* 53 (7) (1984) 2381–2390.
- [49] U.R. Kattner, W.J. Boettinger, *Mater. Sci. Eng. A* 152 (1992) 9–17.
- [50] A. Watson, F.H. Hayes, *J. Alloys Compd.* 320 (2001) 199–206.
- [51] L.E. Tanner, *Phys. Status Solidi* 30 (2) (1968) 685–701.
- [52] T. Massalski, *Binary Alloys Phase Diagrams*, in: *ASM Intl.*, vol. 3, 1992.
- [53] Y. Nunomura, Y. Kaneno, H. Tsuda, T. Takasugi, *Intermetallics* 12 (2004) 239–299.
- [54] W. Soga, Y. Kaneno, T. Takasuga, *Intermetallics* 14 (2006) 170–179.
- [55] X.L. Huang, H.Y. Zhou, Q.R. Yao, Z.M. Wang, *J. Alloys Compd.* 456 (1–2) (2008) 178–180.
- [56] Y. Kamada, M. Matsui, T. Asada, *J. Phys. Soc. Japan* 66 (2) (1997) 466–471.
- [57] Y. Zhu, P. Yu, X. Jin, D.-S. Wang, *J. Magn. Magn. Mater.* 310 (2007) 301–303.
- [58] J.-M. Zhang, H.-T. Li, K.-W. Xu, *Solid State Commun.* 141 (2007) 535–540.
- [59] H.L. Lukas, S. Fries Gomez, B. Sundman, *Computational Thermodynamics, the Calphad Method*, 1st ed., Cambridge University Press, New York, United States of America, 2007.
- [60] M. Hillert, *Phase Equilibria, Phase diagrams and Phase Transformations, Their Thermodynamic basis*, 2nd Edition, Cambridge University Press, New York, United States of America, 2008.
- [61] B. Sundman, CIRIMAT, Al–Fe, 2008, Unpublished published work on Al–Fe.
- [62] C. Servant, B. Sundman, O. Lyon, *CALPHAD* 25 (1) (2001) 79–95.
- [63] I. Ansara, 2000, Unpublished work.
- [64] I. Ansara, 1995, Unpublished work.
- [65] A. Kusoffsky, N. Dupin, B. Sundman, *CALPHAD* 25 (4) (2001) 549–565.
- [66] N. Dupin, I. Ansara, B. Sundman, *CALPHAD* 25 (2) (2001) 279–298.
- [67] Y. Himuro, Y. Tanaka, N. Kamiya, I. Ohnuma, R. Kainuma, K. Ishida, *Intermetallics* 12 (2004) 635–643.
- [68] R.J. Wakelin, E.L. Yates, *Proc. Phys. Soc. (London)*, B 66 (1953) 221–240.
- [69] Y. Mischin, M.J. Mehl, D.A. Papaconstantopoulos, *Acta Mater.* 53 (2005) 4029–4041.
- [70] F. Lechermann, M. Färlhe, J.M. Sanchez, *Intermetallics* 13 (2005) 1096–1109.
- [71] Y. Chen, S. Iwata, T. Mohri, *Rare Metals* 25 (5) (2006) 437–440.
- [72] X.Y. Huang, J.S. Pan, Y.D. Fan, *Solid State Commun.* 104 (2) (1997) 101–105.
- [73] Y. Du, Y.A. Chang, W. Gong, B. Huang, H. Xu, Z. Jin, F. Zhang, S.-L. Chen, *Intermetallics* 11 (2003) 995–1013.
- [74] K.A. Peard, D.W. Borland, *Scripta Metall.* 3 (1969) 267–270.
- [75] K. Leitch, M. Chaturvedi, *Metall. Trans.* 2 (1971) 1407–1413.
- [76] L.A. Panteleimonov, L.V. Aleshina, *Vestn. Mosk. Univ.* 16 (5) (1975) 630.
- [77] K.V. Varli, T.I. Druzhinina, N.P. D'Yakonova, S.E. Pirogova, A.M. Rutman, *Izv. Vysshikh Uchebn. Zaved. Chernaya Metall.* 9 (1981) 116–118.
- [78] Y.A. Skakov, N.P. D'Yakonova, V.V. Savin, V.K. Semina, A.V. Sharshatkina, *Izv. Vysshikh Uchebn. Zaved. Chernaya Metall.* 5 (1985) 85–90.
- [79] T. Ueyama, M.M. Ghanem, N. Miura, M. Takeyama, T. Matsuo, *Thermec'97, International Conference on Thermomechanical Processing of Steels and Others Materials, The Minerals, Metals and Materials Society*, 1997, pp. 1753–1760.
- [80] S. Asano, S. Ishida, *J. Magn. Magn. Mater.* 70 (1987) 39–43.
- [81] J. Miettinen, *CALPHAD* 22 (2) (1998) 275–300.
- [82] N. Saunders, A.P. Miodownik, TTNi6, TT Ni-based Superalloys Database (Version 6.0 Jul. 2003), 2003.
- [83] J. Valdes, D.-E. Kim, S.-L. Shang, X. Liu, P. King, Z.-K. Liu, *Proceeding of the 11th International Symposium Superalloys 2008*, 14–18th September 2008, Champion, PA, USA (unpublished). Available on line at: [http://cms.tms.org/ftp/tmsftp.nsf/0/cd2e2877e6fe37558525740300701e03/\\$FILE/22551.pdf](http://cms.tms.org/ftp/tmsftp.nsf/0/cd2e2877e6fe37558525740300701e03/$FILE/22551.pdf).
- [84] C. Wagner, *Thermodynamic of Alloys*, Addison-Wesley Press, Inc., Cambridge, MA, USA, 1952.
- [85] N. Dupin, Ph.D. Thesis, LTPCM Grenoble, 1995.
- [86] N. Dupin, B. Sundman, *Scand. J. Metall.* 30 (2001) 184–192.
- [87] J.P. Perdew, K. Burke, M. Ernzerhof, *Phys. Rev. Lett.* 78 (1997) 1396.
- [88] Vienna Ab-Initio Simulation Package, Kresse G., J. Furthmüller, Institut für Materialphysik, Universität Wien, Sensengasse 8, A-1130 Wien, Austria. <http://cms.mpi.univie.ac.at/vasp/>.
- [89] G. Kresse, J. Hafner, *Phys. Rev. B* 47 (1) (1993) 558–561.
- [90] G. Kresse, J. Furthmüller, *Comput. Mater. Sci.* 6 (1996) 15–50.
- [91] G. Kresse, J. Furthmüller, *Phys. Rev. B* 54 (1996) 11169–11186.
- [92] G. Kresse, J. Joubert, *Phys. Rev. B* 59 (1999) 1758–1775.
- [93] Y. Wang, S. Curtarolo, C. Jiang, R. Arroyave, T. Wanga, G. Cederc, L.-Q. Chena, Z.-K. Liua, *Comput. Coupling Phase Diagrams Thermochem.* 28 (2004) 79–90.
- [94] P.P. Perdew, Y. Wang, *Phys. Rev. B* 45 (1992) 13244–13249.
- [95] Thermotech Ltd./Sente Software Ltd., Surrey Technology Center, United Kingdom. <http://www.thermotech.co.uk/>.
- [96] M.H.F. Sluiter, *CALPHAD* 30 (2006) 357–366.
- [97] L.T. Kong, B.X. Liu, *J. Alloys Compd.* 414 (2006) 36–41.
- [98] G. Inden, *Proc. Project Meeting Calphad V, Düsseldorf*, 1976, III.4-1.
- [99] M. Hillert, M. Jarl, *CALPHAD* 2 (1978) 227–238.
- [100] J.H. Xu, T. Oguchi, A.J. Freeman, *Phys. Rev. B* 35 (13) (1987) 6940–6943.
- [101] Y. Du, S. Liu, Y.A. Chang, Y. Yang, *CALPHAD* 29 (2005) 140–148.